

Clustering without geometry in sparse networks with independent edges

Alessio Catanzaro^{1,2,3}, Remco van der Hofstad⁴, and Diego Garlaschelli^{1,2}

¹*IMT School for Advanced Studies, Lucca, Italy*

²*Instituut-Lorentz for Theoretical Physics, Leiden University, The Netherlands*

³*Università di Palermo, Palermo, Italy and*

⁴*Department of Mathematics and Computer Science,
Eindhoven University of Technology, The Netherlands.*

(Dated: March 16, 2026)

The coexistence of sparsity and clustering (non-vanishing average fraction of triangles per node) is one of the few structural features that, irrespective of finer details, are ubiquitously observed across large real-world networks. This fact calls for generic models producing sparse clustered graphs. Earlier results suggested that sparse random graphs with independent edges fail to reproduce clustering, unless edge probabilities are assumed to depend on underlying metric distances that, thanks to the triangle inequality, naturally favour triadic closure. This observation has opened a debate on whether clustering implies (latent) geometry in real-world networks. Alternatively, recent models of higher-order networks can replicate clustering by abandoning edge independence. In this paper, we mathematically prove, and numerically confirm, that a sparse random graph with independent edges, recently identified in the context of network renormalization as an invariant model under node aggregation, produces finite clustering without any geometric or higher-order constraint. The underlying mechanism is an infinite-mean node fitness, which also implies a power-law degree distribution. Further, as a novel phenomenon that we characterize rigorously, we observe the breakdown of self-averaging of various network properties. Therefore, as an alternative to geometry or higher-order dependencies, node aggregation invariance emerges as a basic route to realistic network properties.

Introduction: clustering versus geometry. While real-world networks differ in various structural details, the vast majority of them are characterized by virtually ubiquitous features, the most popular of which are the broad (i.e., infinite-variance) distribution of node degrees (numbers of links per node), the (*ultra*)*small-world* property (i.e., average shortest path length growing (at most) logarithmically with the number of nodes), and the coexistence of *sparsity* (i.e., vanishing link density) and *local clustering* (i.e., finite average density of triangles around nodes) in the limit of infinitely large networks [1, 2]. While several models based on different generic mechanisms can successfully replicate broad degree distributions and short path lengths [2, 3], the coexistence of sparsity and local clustering is much more difficult to replicate – and hence more informative, as it requires specific mechanisms that can discriminate models at a finer level.

The prototypical example of this difficulty is illustrated by *random graph models with independent edges*, where different pairs of nodes are independently connected. In the Erdős-Rényi (ER) model [4], where edges are independent and identically distributed (i.i.d.) with the same connection probability p , it is easy to show that the link density (expected fraction of realized links) and the local clustering coefficient (defined as the fraction of triangles around a node, averaged over all nodes) have the same expected value p for networks with a large number n of nodes. This automatically implies that, as n diverges, one cannot simultaneously produce finite local clustering and vanishing link density. To overcome this limitation of the ER model, two main routes have been explored.

One route introduces dependencies between edges.

This can happen via the addition of explicit triadic interactions in an Exponential Random Graph setting [5, 6] (which may however still lead to comparable levels of density and clustering), the random superposition of small subgraphs [7] or the monopartite projection [8] of random bipartite networks [9] – both producing networks of overlapping cliques (the edges of which are all mutually dependent) where local clustering can remain very large even for vanishing density. More recent attempts generalize these ideas to higher-order networks such as simplicial complexes and hypergraphs [10, 11], where edges belonging to the same simplex or hyperedge are mutually dependent. While these more complicated settings can realize the coexistence of sparsity and clustering at the expense of introducing higher-order dependencies, whether that coexistence can be achieved for more parsimonious models with independent edges remains an open question.

The second route explores that question explicitly by preserving edge independence while introducing heterogeneity. More precisely, one can turn the *unconditional* link independence of the ER model into a *conditional* one, by replacing, for each specific pair of nodes i and j ($i, j = 1, \dots, n$), the constant connection probability p with a probability p_{ij} that is a function $f(w_i, w_j)$ of the realized values w_i, w_j of a certain node-specific variable w (called *fitness* or weight, hidden variable, latent variable, Lagrange multiplier, etc.) that is preliminarily assigned to vertices via an i.i.d. draw from a certain probability density function (pdf) $\rho(w)$ [3, 12–14]. Typical choices of $f(w_i, w_j)$ are monotonically increasing in both arguments (and necessarily symmetric for undirected graphs) – implementing the idea that, the larger the fitness, the larger the probability that a node connects to other nodes [15].

In the studies carried out so far, it turned out that, while several combinations of f and ρ can generate sparse small-world networks with a broad degree distribution [3, 12–14], they systematically fail to generate (positive) clustering, casting doubts on whether models with independent edges can replicate local clustering. The only exception that has become popular is that of *random geometric graphs*, where the fitness w acquires the role of a *node coordinate* (which, more generally, can be a D -dimensional vector), and the connection function f depends on w_i and w_j through some *metric distance* $d_{ij} = d(w_i, w_j)$ (in which case, f generally loses the property of being monotonic in w_i [16]). A remarkable example of this success is the *hyperbolic model* [6, 17–23], which assumes that nodes are sprinkled uniformly at random in a D -dimensional hyperbolic space and links are formed with a probability that is a certain decreasing function of the geodesic distance between nodes. In this setting, the triangle inequality ($d_{ij} \leq d_{ik} + d_{jk} \forall i, j, k$) guarantees that pairs of nodes i, j that successfully connect to a third node k are very likely to connect to each other (*triadic closure*), provably leading to positive clustering [24, 25]. Additionally, hyperbolicity ensures that other desirable properties such as power-law degree distributions emerge [22]. These investigations have convincingly concluded that, in random graphs with conditionally independent edges and distance-dependent connection probabilities, *geometry implies clustering*.

On the other hand, the potential reverse (non-obvious) implication that *clustering implies geometry*, i.e., that the presence of finite clustering could suffice to indicate that the network is (with high probability) the realization of a random geometric graph, is highly debated [6, 17–23]. Whether clustering implies geometry is crucial for network theory (because, if true, it would demand for explanations and interpretations of the hidden geometry of real-world networks [21, 24]), for data science (for instance because techniques such as graph embedding and topological data analysis could then be optimized for real-world network geometries), and for the control of processes on networks (because geometry could aid network navigability [22, 26, 27], and the understanding of how clustering impacts epidemic and other processes [5]).

In this Letter, we prove that positive clustering can emerge *independently* of geometry or higher-order constraints in random graphs with independent edges conditional on infinite-mean fitness [28, 29]. While the finite-mean case has been systematically found to produce vanishing clustering, we show that in the infinite-mean case clustering is positive and strong. Notably, we find that the infinite-mean fitness also implies the breakdown of self-averaging in certain properties, including clustering itself.

The Multi-Scale Model. We consider the inhomogeneous random graph model introduced in [28] and studied in [29–31]. Each node i is assigned a positive weight (fitness) w_i ($i = 1, \dots, n$), sampled i.i.d. from a certain pdf $\rho(w)$. Given w_i, w_j , nodes i, j connect with proba-

bility

$$p_{ij} = 1 - e^{-\delta_n w_i w_j}, \quad (1)$$

where the scaling δ_n can be chosen in such a way that the link density vanishes as $n \rightarrow \infty$. The connection probability (1) is also known in the literature as the Norros–Reittu model [32] and has been used for various purposes [33, 34], by considering a finite-mean $\rho(w)$. In this work we are however interested in the specific ‘annealed’ regime considered within the framework of network renormalization [35], where the model emerges as a fixed point of a renormalization flow in the space of models, induced by coarse-graining the network by aggregating nodes into super-nodes and recalculating the induced connection probability between super-nodes [28]. The specific connection rule in (1) makes the model invariant, provided the weight of each block is defined as (a random variable equal to) the sum of the weights of the constituent nodes [28]. If one further demands the invariance of the weight distribution, i.e., that the coarse-grained weights are distributed according to the same pdf as the constituent weights, then $\rho(w)$ should be a positively-supported, one-sided α -stable law $\tilde{\rho}_\alpha(w)$ with stability parameter $0 < \alpha < 1$ [36, 37] and tails decaying as $w^{-1-\alpha}$ for large w , hence with diverging mean and higher moments [28, 30]. In this way, one gets a Multi-Scale Model (MSM) interpretable as describing connections between arbitrarily nested (blocks of) nodes, thereby describing the graph at multiple scales of resolution (coarse-graining) simultaneously [28].

Since a stable law $\tilde{\rho}_\alpha(w)$ with $0 < \alpha < 1$ is known in closed form only for $\alpha = \frac{1}{2}$ (Lévy distribution), we first follow [30] and replace it with a pure Pareto distribution

$$\rho_\alpha(w) = \alpha w^{-1-\alpha}, \quad w \geq 1, \quad 0 < \alpha < 1, \quad (2)$$

(which has exactly the same tail behaviour as an α -stable distribution and serves as an analytically tractable counterpart [30, 36]) and then discuss the extension to actual α -stable laws $\tilde{\rho}_\alpha(w)$ via both analytical and numerical arguments. Given (2), one can show that choosing $\delta_n = n^{-1/\alpha}$ implies that the link density vanishes as $\log n/n$, i.e., the average degree grows only as $\log n$, and the degree distribution is power-law [30].

We stress that the MSM can be enriched with additional dyadic features [28, 29] which allow the connection probabilities to depend, for instance, on geometric distances between coordinates assigned to nodes. Nonetheless, to investigate whether clustering can be produced *without* geometry, here we obviously consider the simplest, distance-independent version in (1).

The Local Clustering Coefficient. Abstractly, the clustering coefficient quantifies the tendency of a graph to form closed triangles. Globally, it can be defined as the ratio between the total number of closed triangles and the number of potential (either open or closed) triangles (also called cherries, or wedges). In our regime with $0 < \alpha < 1$, this ratio vanishes for the MSM model [30], in

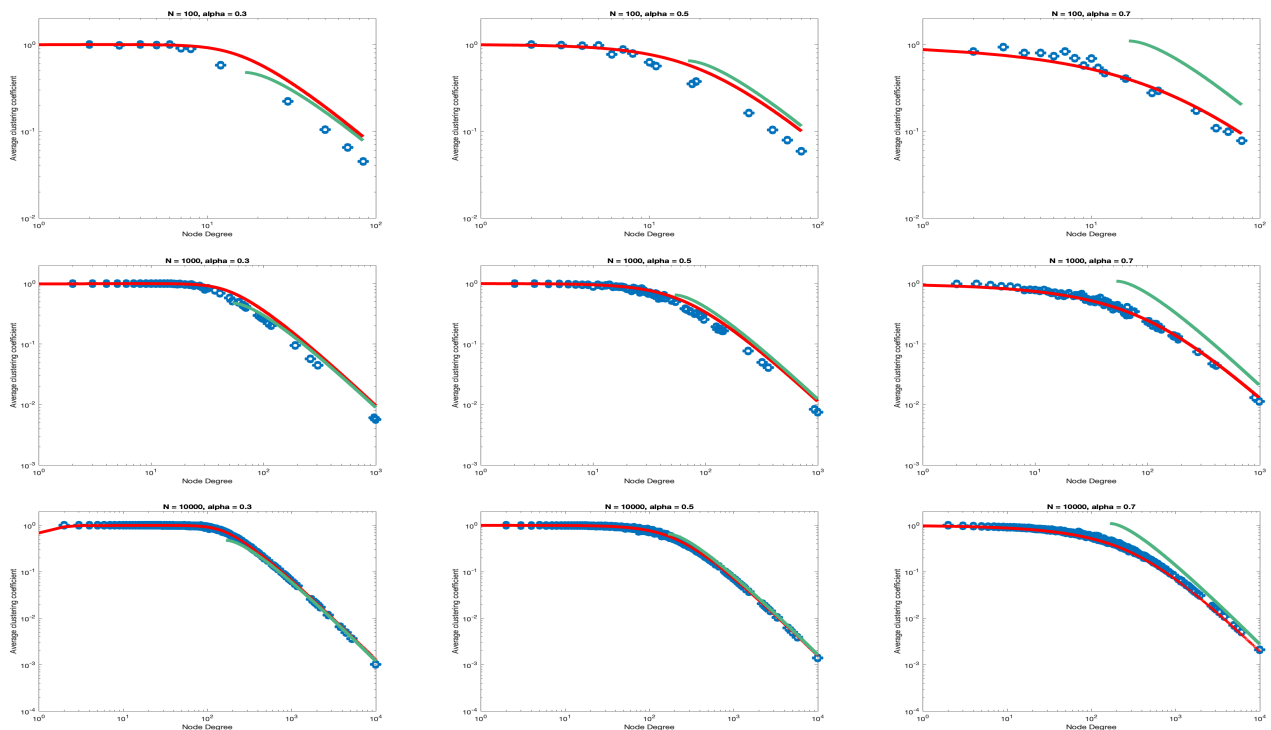


FIG. 1: **Clustering functions for different values of n and α for the MSM model (1) with Pareto weights (2).** Blue circles: empirical clustering function (4) (versus the reduced degree $a = k/\sqrt{n}$) computed on actual realized graphs sampled from the model (obtained by sampling the weights once, and sampling the graph once conditionally on the realized weights). Red curves: our analytical expression (6) for the annealed clustering function. Green curves: our asymptotic calculation (8) valid for diverging reduced degrees. We evaluate and plot all functions only for degrees larger than 1, to avoid ambiguities in the definition of the clustering coefficient for $k < 2$. From top to bottom: $n = 10^2, 10^3, 10^4$. From left to right: $\alpha = 0.3, 0.5, 0.7$.

line with what is observed in sparse real-world networks. Our interest here is the (more distinctive) *local* clustering coefficient C_v , which quantifies the tendency of the neighbours of the specific node v to form closed triangles around v . For a node v with degree D_v , C_v is defined as the ratio between the number Δ_v of triangles containing v and the number of wedges centered at v . In terms of the adjacency matrix $A = (A_{ij})_{i,j=1}^n$, this reads

$$C_v = \frac{\Delta_v}{\binom{D_v}{2}} = \frac{\sum_{i \neq v} \sum_{j \neq v, i} A_{vi} A_{ij} A_{jv}}{D_v(D_v - 1)}, \quad D_v > 1. \quad (3)$$

The behaviour of C_v versus D_v , as well as the average value C of C_v over nodes, can effectively characterize real-world networks and discriminate among different models – especially in determining whether a finite (expected) value of C can emerge in large sparse graphs, as observed in real-world networks. Note that C_v in (3) is defined only for nodes with $D_v > 1$, as only nodes with at least two neighbours can host a triangle. For nodes with $D_v = 0, 1$, one can either leave C_v undefined (and exclude it from the calculation of C) or conventionally set $C_v \equiv 0$ (and include it in the calculation of C). We will consider both cases and discuss their implications.

Clustering Function. For a given graph, we consider the average clustering coefficient as a function of the degree k of each node, i.e., the *empirical clustering function*

$$C(k) = \frac{1}{N_k} \sum_{v: D_v=k} \frac{\Delta_v}{\binom{k}{2}}, \quad (4)$$

where $N_k = \sum_{v: D_v=k} \delta_{D_v,k}$ is the number of nodes with degree k . In terms of expectations (\mathbb{E}) over the model, we introduce the *annealed clustering function* as

$$\bar{C}(k) = \frac{1}{\mathbb{E}[N_k]} \mathbb{E} \left[\sum_{v: D_v=k} \frac{\Delta_v}{\binom{k}{2}} \right]. \quad (5)$$

One of our main results is a rigorous calculation of $\bar{C}(k)$ in the asymptotic (large n) limit, valid for both small and large k , which shows excellent agreement with the empirical clustering function $C(k)$ [38]. In this setting, we redefine $\bar{C}(\cdot)$ as a function of the *reduced degree* $a = k/\sqrt{n}$, as this rescaling allows us to prove that, defining $g(x) \equiv 1 - e^{-x}$, the limiting form of $\bar{C}(a)$ as $n \rightarrow \infty$ is

$$\bar{C}(a) = \frac{\alpha^2}{a^2} \int_0^\infty dx \int_0^\infty dy \frac{g(a^{1/\alpha} \tau_\alpha x) g(a^{1/\alpha} \tau_\alpha y)}{x^{1+\alpha} y^{1+\alpha}} g(xy), \quad (6)$$

where $\tau_\alpha \equiv \Gamma(1 - \alpha)^{-1/\alpha}$, and $\Gamma(\cdot)$ is the Euler Gamma function. The proof is in Supplementary Information (SI). In Figure 1, we compare the numerical evaluation of the integral (6) with the direct computation of the empirical clustering function (4) on the actual realizations of the random graph. The agreement is remarkably good, already for moderate values of n .

Hub and Leaf Behaviour. To refine the characterization of clustering in the model, we investigate the limiting behavior of the annealed clustering function for nodes in two distinct regimes of the degree spectrum: *leaf* and *hub* nodes, corresponding to poorly and highly connected ones, respectively. For leaf (L) nodes, defined as nodes with vanishing reduced degree $a \rightarrow 0$, we find (see SI) that the function in (6) has the asymptotic plateau

$$\bar{C}_L \equiv \lim_{a \rightarrow 0} \bar{C}(a) = 1, \quad (7)$$

which implies that in the low-degree limit the local neighborhood of a node is almost fully clustered (excluding of course nodes with $k = 0, 1$). For hub (H) nodes, defined as nodes with diverging reduced degree $a \rightarrow \infty$, we find (see SI) that the function (6) decays as

$$\bar{C}(a) \sim \bar{C}_H(a) \equiv 2\Gamma(1 - \alpha) \frac{\log a}{a^2}, \quad a \rightarrow \infty. \quad (8)$$

Figure 1 shows that the asymptotics (7) and (8) are in excellent agreement both with the empirical clustering function (4) computed on actual realizations of the random graph and with the full analytical expression (6) for the annealed clustering function (5).

Average Clustering Coefficient. The previous results finally allow us to estimate the overall expected value \bar{C} of the average local clustering coefficient C by averaging the annealed clustering function $\bar{C}(a)$ over the distribution $P(a)$ of the reduced degree a as

$$\begin{aligned} \bar{C} &\equiv \int da \bar{C}(a)P(a) \\ &\simeq \int_{a \in L} da \bar{C}_L(a)P(a) + \int_{a \in H} da \bar{C}_H(a)P(a), \end{aligned} \quad (9)$$

where we have formally split the integral into two contributions, produced by leaf ($a \in L$) and hub ($a \in H$) nodes respectively, consistent with the two regimes characterized asymptotically in (7) and (8). A rigorous definition of this split is provided in SI, where we also show that, in order to compute \bar{C} exactly, it is not necessary to identify precisely the crossover value(s) of a separating the two regions. Notably, it turns out that the integral over $a \in H$ in (9) vanishes, implying that hubs do not contribute to the overall clustering (see SI). The remaining contribution of the leaf nodes $a \in L$ is always finite, but its precise value depends on whether C_k for nodes with degree $k < 2$ is defined as $C_{k < 2} \equiv 0$ and hence included in the integration over L (in which case $\bar{C}_L(a) \equiv 0$ for $0 \leq a \leq 1/\sqrt{n}$) or undefined and not included in the

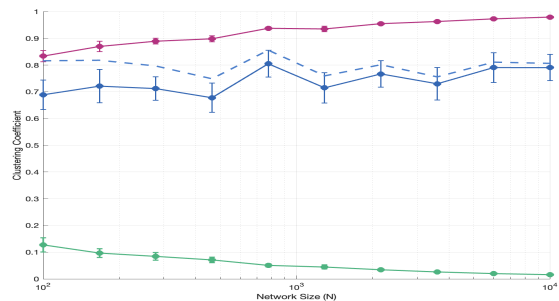


FIG. 2: **Average local clustering coefficient C and distance to $r_{0/1}$ versus network size n (for $\alpha = 0.5$).** All results are obtained by sampling the weights 10 times independently for each value of n , sampling a single graph conditionally on each realization of the weights, computing the relevant quantities on that single graph, and finally calculating averages and error bars over the 10 realizations. The trends show the node-averaged local clustering coefficient C , both including (blue symbols) and excluding (purple symbols) nodes with degree $k < 2$: note that the latter evolves smoothly towards 1 with shrinking error bars as n increases, while the former fluctuates with non-vanishing error bars (as a result of non-self-averaging) and becomes progressively closer to $1 - r_{0/1}$ over realizations (dashed blue line), which is also fluctuating. The difference between $1 - r_{0/1}$ and C computed including nodes with $k < 2$ (green symbols) converges to zero with shrinking error bars.

integration. In SI we find that, depending on the choice,

$$\lim_{n \rightarrow \infty} \bar{C} = \begin{cases} 1 & \text{if } C_{k < 2} \text{ undefined,} \\ 1 - r_{0/1} & \text{if } C_{k < 2} \equiv 0, \end{cases} \quad (10)$$

where $r_{0/1}$ is the expected fraction of nodes with degree 0 or 1. We plot the two versions of the average local clustering coefficient in Figure 2, confirming the agreement with the theoretical calculations. This result means that the network is strongly clustered: for almost all nodes that can form triangles, almost all triangles are closed.

Lack of Self-Averaging. The result (10) is calculated conditionally on the realized weights $\{w_i\}_{i=1}^n$. It shows that, if nodes with $k < 2$ are excluded, \bar{C} converges to the (deterministic) maximum value 1, with vanishing fluctuations. By contrast, as we show in SI, for finite but large n , the fractions of nodes with degree zero and one concentrate around functions of the rescaled total weight $S_n = \delta_n \sum_{j=1}^n w_j$, which in turn converges in distribution to an α -stable random variable, and thus remains a fluctuating quantity. This means that, for given n and α , different realizations of the weights produce different values of $r_{0/1}$ and of \bar{C} , if nodes with $k < 2$ are included. Therefore, under this second definition, \bar{C} converges in distribution to the random variable $1 - r_{0/1}$, remaining macroscopically fluctuating even in the large graph

limit. This behaviour follows from the infinite-mean nature of the weights and is a notable manifestation of the (rather unique) lack of self-averaging in macroscopic network properties (the fractions of nodes with $k < 2$, and \bar{C} itself), which is not typically observed in models with independent edges and finite-mean weights. All these results are proven in SI and confirmed numerically in Figure 2.

Concluding Remarks. This Letter contributes to the open debate about whether, in models with conditionally independent edges, the coexistence of sparsity and local clustering (along with other desirable features such as a broad degree distribution and the small-world property) can be attained *without geometry*, i.e., without assuming that the connection probability p_{ij} depends on the node attributes w_i and w_j necessarily through a function of some metric distance $d(w_i, w_j)$ [6, 17–24]. We considered a geometry-free model with independent edges and infinite-mean fitness [28, 29], recently introduced in the context of network renormalization [35], and calculated its full clustering function – rigorously proving the resulting *finite* local clustering in the large n limit and highlighting that clustering does *not* imply geometry. The infinite-mean nature of the fitness arises from a requirement of model invariance under node aggregation [28] and generates other realistic properties including sparsity, a power-law degree distribution [29], and the breakdown of self-averaging of various network properties (in-

cluding the fraction of isolated nodes and its contribution to the average clustering itself), which is a novel result characterized here. The model then exposes, as an alternative to geometry, the hypothesis of node aggregation invariance as a basic candidate mechanism producing realistic network properties.

Acknowledgments This publication is part of the projects “Network renormalization: from theoretical physics to the resilience of societies” with file number NWA.1418.24.029 of the research programme NWA L3 - Innovative projects within routes 2024, which is (partly) financed by the Dutch Research Council (NWO) under the grant <https://doi.org/10.61686/A0IJP05368>, and “Redefining renormalization for complex networks” with file number OCENW.M.24.039 of the research programme Open Competition Domain Science Package 24-1, which is (partly) financed by the Dutch Research Council (NWO) under the grant <https://doi.org/10.61686/PBSEC42210>. The work of van der Hofstad is supported in part by the Netherlands Organisation for Scientific Research (NWO) through the Gravitation NETWORKS grant 024.002.003. Early interactions between RvdH and DG took place between 29 January and 02 February 2024 during the ICTS-NETWORKS workshop “Challenges in Networks” (ICTS-NETWORKS2024/01) at the International Centre for Theoretical Sciences (ICTS-TIFR) in Bangalore, India.

-
- [1] G. Caldarelli, *Scale-free networks: complex webs in nature and technology* (Oxford University Press, 2007).
- [2] M. Newman, *Networks* (Oxford university press, 2018).
- [3] R. Van Der Hofstad, *Random graphs and complex networks: Volume 1* (2016).
- [4] P. Erdős, A. Rényi, *et al.*, On the evolution of random graphs, *Publ. Math. Inst. Hungar. Acad. Sci.* (1960).
- [5] M. E. Newman, Properties of highly clustered networks, *Physical Review E* **68**, 026121 (2003).
- [6] M. E. Newman, Random graphs with clustering, *Physical review letters* **103**, 058701 (2009).
- [7] B. Bollobás, S. Janson, and O. Riordan, Sparse random graphs with clustering, *Random Structures & Algorithms* **38**, 269 (2011).
- [8] In monopartite projections of bipartite networks, the original nodes are first initially connected (possibly independently of each other) to ‘auxiliary’ nodes of a different type (representing for instance the possible affiliations or memberships of the original nodes), and the auxiliary nodes are then eliminated while connecting the original nodes to each other, if they share connections to the same auxiliary nodes.
- [9] M. E. Newman and J. Park, Why social networks are different from other types of networks, *Physical review E* **68**, 036122 (2003).
- [10] F. Battiston and G. Petri, *Higher-order systems* (Springer, 2022).
- [11] S. Boccaletti, P. De Lellis, C. Del Genio, K. Alfaro-Bittner, R. Criado, S. Jalan, and M. Romance, The structure and dynamics of networks with higher order interactions, *Physics Reports* **1018**, 1 (2023).
- [12] G. Caldarelli, A. Capocci, P. De Los Rios, and M. A. Munoz, Scale-free networks from varying vertex intrinsic fitness, *Physical review letters* **89**, 258702 (2002).
- [13] M. Boguná and R. Pastor-Satorras, Class of correlated random networks with hidden variables, *Physical Review E* **68**, 036112 (2003).
- [14] T. Squartini and D. Garlaschelli, *Maximum-entropy networks: Pattern detection, network reconstruction and graph combinatorics* (Springer, 2017).
- [15] Some popular examples are $f(w_i, w_j) = zw_iw_j$, $f(w_i, w_j) = \Theta(w_i + w_j - z)$, $f(w_i, w_j) = zw_iw_j/(1 + zw_iw_j)$, and $f(w_i, w_j) = 1 - e^{-zw_iw_j}$, where $z > 0$ is a global parameter controlling for the overall link density and $w_i \geq 0 \forall i$.
- [16] For instance, if w_i and w_j are scalar (one-dimensional) coordinates and their distance is defined as $d_{ij} = |w_i - w_j|$, then w_i and w_j can simultaneously increase while keeping d_{ij} (and hence p_{ij}) unchanged.
- [17] D. Krioukov, Clustering implies geometry in networks, *Physical review letters* **116**, 208302 (2016).
- [18] R. Aliakbarisani, M. Boguñá, and M. Á. Serrano, Clustering does not always imply latent geometry, *Physical Review Letters* **135**, 197402 (2025).
- [19] M. Á. Serrano and M. Boguna, Clustering in complex networks. i. general formalism, *Physical Review E—Statistical, Nonlinear, and Soft Matter Physics* **74**, 056114 (2006).

- [20] M. Á. Serrano and M. Boguná, Clustering in complex networks. ii. percolation properties, *Physical Review E—Statistical, Nonlinear, and Soft Matter Physics* **74**, 056115 (2006).
- [21] M. Boguna, I. Bonamassa, M. De Domenico, S. Havlin, D. Krioukov, and M. Á. Serrano, Network geometry, *Nature Reviews Physics* **3**, 114 (2021).
- [22] D. Krioukov, F. Papadopoulos, M. Kitsak, A. Vahdat, and M. Boguná, Hyperbolic geometry of complex networks, *Physical Review E—Statistical, Nonlinear, and Soft Matter Physics* **82**, 036106 (2010).
- [23] R. Michielan, N. Litvak, and C. Stegehuis, Detecting hyperbolic geometry in networks: Why triangles are not enough, *Physical Review E* **106**, 054303 (2022).
- [24] A. Allard, M. Á. Serrano, and M. Boguná, Geometric description of clustering in directed networks, *Nature Physics* **20**, 150 (2024).
- [25] E. Candellero and N. Fountoulakis, Clustering and the hyperbolic geometry of complex networks, in *Algorithms and Models for the Web Graph: 11th International Workshop, WAW 2014, Beijing, China, December 17-18, 2014, Proceedings 11* (Springer, 2014) pp. 1–12.
- [26] M. Boguna, D. Krioukov, and K. C. Claffy, Navigability of complex networks, *Nature Physics* **5**, 74 (2009).
- [27] M. Boguná, F. Papadopoulos, and D. Krioukov, Sustaining the internet with hyperbolic mapping, *Nature communications* **1**, 62 (2010).
- [28] E. Garuccio, M. Lalli, and D. Garlaschelli, Multiscale network renormalization: Scale-invariance without geometry, *Physical Review Research* **5**, 043101 (2023).
- [29] M. Lalli and D. Garlaschelli, Geometry-free renormalization of directed networks: scale-invariance and reciprocity, *arXiv preprint arXiv:2403.00235* (2024).
- [30] L. Avena, D. Garlaschelli, R. S. Hazra, and M. Lalli, Inhomogeneous random graphs with infinite-mean fitness variables, *Journal of Applied Probability* , 1–26 (2025).
- [31] A. Catanzaro, R. S. Hazra, and D. Garlaschelli, Spectra of random graphs with discrete scale invariance, *arXiv preprint arXiv:2509.12407* (2025).
- [32] I. Norros and H. Reittu, On a conditionally poissonian graph process, *Advances in Applied Probability* **38**, 59 (2006).
- [33] G. J. Rodgers, K. Austin, B. Kahng, and D. Kim, Eigenvalue spectra of complex networks, *Journal of Physics A: Mathematical and General* **38**, 9431 (2005).
- [34] S. Bhamidi, R. van der Hofstad, and J. van Leeuwen, Scaling limits for critical inhomogeneous random graphs with finite third moments, *Electronic Journal of Probability* **15**, 1682 (2010).
- [35] A. Gabrielli, D. Garlaschelli, S. P. Patil, and M. Serrano, Network renormalization, *Nature Reviews Physics* **7**, 203 (2025).
- [36] G. Samorodnitsky and M. S. Taqqu, *Stable non-Gaussian random processes: stochastic models with infinite variance*, Vol. 1 (CRC press, 1994).
- [37] J. Nolan, *Univariate stable distributions: models for heavy tailed data*, Springer Series in Operations Research and Financial Engineering (Springer, Cham, [2020] ©2020) pp. xv+333.
- [38] We also believe that, through a second-moment analysis, it could be proven that in the large n limit, with high probability, the two clustering functions become the same. We will however not prove this claim in the present work.
- [39] R. Leipus, J. Šiaulyš, and D. Konstantinides, *Closure properties for heavy-tailed and related distributions—an overview*, SpringerBriefs in Statistics (Springer, Cham, 2023) pp. ix+92.
- [40] B. Bollobás, W. Fulton, A. Katok, *et al.*, Cambridge studies in advanced mathematics, in *Random graphs* (Cambridge University Press Cambridge, UK, 2001).
- [41] S. Janson, T. Łuczak, and A. Ruciński, Wiley-intercience series in discrete mathematics and optimization, in *Random Graphs* (2000).
- [42] R. Van Der Hofstad, *Random graphs and complex networks, : Volume 2* (Cambridge university press, 2024).
- [43] H. Van Den Esker, R. Van Der Hofstad, G. Hooghiemstra, and D. Znamenski, Distances in random graphs with infinite mean degrees, *Extremes* **8**, 111 (2005).
- [44] A. Baptista, R. J. Sánchez-García, A. Baudot, and G. Bianconi, Zoo guide to network embedding, *Journal of Physics: Complexity* **4**, 042001 (2023).
- [45] M. Ballerini, N. Cabibbo, R. Candelier, A. Cavagna, E. Cisbani, I. Giardina, V. Lecomte, A. Orlandi, G. Parisi, A. Procaccini, *et al.*, Interaction ruling animal collective behavior depends on topological rather than metric distance: Evidence from a field study, *Proceedings of the national academy of sciences* **105**, 1232 (2008).
- [46] R. Van Der Hofstad, G. Hooghiemstra, and D. Znamenski, Random graphs with arbitrary iid degrees, *arXiv preprint math/0502580* (2005).
- [47] D. J. Watts and S. H. Strogatz, Collective dynamics of ‘small-world’ networks, *nature* **393**, 440 (1998).

SUPPLEMENTARY INFORMATION

accompanying the paper

“Clustering without geometry in sparse networks with independent edges”

by A. Catanzaro, R. van der Hofstad and D. Garlaschelli

S.I. ANNEALED CLUSTERING FUNCTION

Theorem 1. *Let the vertex space of the network be $[n] = \{1, \dots, n\}$. Let $(W_v)_{v \in [n]}$ be i.i.d. Pareto random variables, so that their density equals*

$$\rho_\alpha(w) = \frac{\alpha}{w^{\alpha+1}}, \quad w \geq 1, \quad (\text{S1})$$

with $\alpha \in (0, 1)$, so that $\mathbb{E}[W] = \infty$. Conditionally on $(W_v)_{v \in [n]}$, edges are present independently, with the edge between $u, v \in [n]$ being present with probability

$$p_{uv} = 1 - e^{-W_u W_v / n^{1/\alpha}}. \quad (\text{S2})$$

Throughout, we let $(I_{u,v})_{1 \leq u < v \leq n}$ denote the edge indicator variables (or the elements of the adjacency matrix), so that

$$\mathbb{P}(I_{u,v} = 1 \mid (W_v)_{v \in [n]}) = 1 - e^{-W_u W_v / n^{1/\alpha}}, \quad (\text{S3})$$

and $(I_{u,v})_{1 \leq u < v \leq n}$ are conditionally independent given $(W_v)_{v \in [n]}$. Let the Annealed Clustering Function be defined as

$$\bar{C}(k) = \frac{1}{\mathbb{E}[N_k]} \mathbb{E} \left[\sum_{v/D_v=k} \frac{\Delta_v}{\binom{k}{2}} \right] \quad (\text{S4})$$

Then, as $n \rightarrow \infty$, for $k = a\sqrt{n}$,

$$\bar{C}_n(a\sqrt{n}) \rightarrow \bar{C}(a) = \frac{a^2}{a^2} \int_0^\infty \int_0^\infty [1 - e^{-xa^{1/\alpha}\tau_\alpha}][1 - e^{-ya^{1/\alpha}\tau_\alpha}][1 - e^{-xy}](xy)^{-(\alpha+1)} dx dy, \quad (\text{S5})$$

where $\tau_\alpha = \Gamma(1 - \alpha)^{-1/\alpha}$.

Proof. We compute

$$\mathbb{E}[N_k] = n \mathbb{E} [\mathbb{P}(D_1 = k \mid W_1)], \quad (\text{S6})$$

where we note that, conditionally on $W_1 = w$, $D_1 \sim \text{Bin}(n-1, q_w)$, where

$$q_w = \mathbb{E} [1 - e^{-wW/n^{1/\alpha}}]. \quad (\text{S7})$$

We also compute the numerator

$$\mathbb{E} \left[\sum_{v \in [n]} \Delta_v \mathbb{1}_{D_v=k} \right] = n \mathbb{E} \left[\mathbb{E} [\Delta_1 \mathbb{1}_{D_1=k} \mid W_1] \right] = n \binom{n-1}{2} \mathbb{E} \left[\mathbb{P}(D'_1 = k-2 \mid W_1) \mathbb{P}(I_{1,2} I_{1,3} I_{2,3} = 1 \mid W_1) \right], \quad (\text{S8})$$

where $D'_1 \sim \text{Bin}(n-3, q_w)$, and we have used conditional independence. Here, we can identify

$$D'_1 = \sum_{u \in [n] \setminus \{3\}} I_{1,u}. \quad (\text{S9})$$

We see that all these expectations involve binomial random variables, which we continue to investigate, starting with the conditional success probability q_w .

S.I.i. Analysis of success probabilities

We compute

$$\begin{aligned}
q_w &= \mathbb{E} [1 - e^{-wW/n^{1/\alpha}}] \\
&= \int_1^\infty [1 - e^{-ws/n^{1/\alpha}}] \frac{\alpha}{s^{\alpha+1}} ds = \left(\frac{w}{n^{1/\alpha}}\right)^\alpha \int_{wn^{-1/\alpha}}^\infty [1 - e^{-s}] \frac{\alpha}{s^{\alpha+1}} ds \\
&= \frac{w^\alpha}{n} \int_0^\infty [1 - e^{-s}] \frac{\alpha}{s^{\alpha+1}} ds - \frac{w^\alpha}{n} \int_0^{wn^{-1/\alpha}} [1 - e^{-s}] \frac{\alpha}{s^{\alpha+1}} ds.
\end{aligned} \tag{S10}$$

We next use that

$$\int_0^\infty [1 - e^{-s}] \frac{\alpha}{s^{\alpha+1}} ds = \int_0^\infty \int_0^s e^{-y} dy \frac{\alpha}{s^{\alpha+1}} ds = \int_0^\infty e^{-y} \int_y^\infty \frac{\alpha}{s^{\alpha+1}} ds dy = \int_0^\infty e^{-y} y^{-\alpha} dy = \Gamma(1 - \alpha), \tag{S11}$$

and

$$\int_0^{wn^{-1/\alpha}} [1 - e^{-s}] \frac{\alpha}{s^{\alpha+1}} ds \leq \int_0^{wn^{-1/\alpha}} \frac{\alpha}{s^\alpha} ds = \frac{\alpha}{\alpha - 1} (wn^{-1/\alpha})^{1-\alpha} = \frac{\alpha}{\alpha - 1} w^{1-\alpha} n^{1-1/\alpha}. \tag{S12}$$

This gives excellent control over q_w for all $w = o(n^{1/\alpha})$.

S.I.ii. Binomial local limit approximations

Let $S_m \sim \text{Bin}(m, p)$. Then, a local central limit approximation shows that

$$\mathbb{P}(S_m = k) = \frac{1}{\sqrt{2\pi mp(1-p)}} e^{-(k-mp)^2/[2mp(1-p)]} (1 + o(1)), \tag{S13}$$

when $|k - mp| = o((mp)^{2/3})$, and uniformly in k and p . Such approximations have a long history, we refer to the books by Bollobás [40] and Janson, Łuczak and Ruciński [41]. In particular, the upper bound in (S13) follows from [40, Theorem 1.2], the lower bound from [40, Theorem 1.5], and an analysis of the error terms present there, showing that they are $o(1)$ when $|n - mp| = o((mp)^{2/3})$.

In our case, we have that $m = n - 1$ or $m = n - 2$, $p = q_w$ with $w = W_1$, so that

$$\mathbb{P}(D_1 = k \mid W_1 = w) = \frac{1}{\sqrt{2\pi mq_w(1-q_w)}} e^{-(k-mq_w)^2/[2mq_w(1-q_w)]} (1 + o(1)), \tag{S14}$$

when $|k - mq_w| = o((mq_w)^{2/3})$, and uniformly in k and w . Since, for us, k is fixed, while w is being integrated out over, the above means that the main contribution for $W_1 = w$ comes from w for which $mq_w \approx k$, with values of w for which

$$|k - mq_w| \geq C\sqrt{k} \log k \tag{S15}$$

receiving probability at most

$$e^{-C \log k} = k^{-C}, \tag{S16}$$

which is negligible. Thus, we can safely think of $mq_w = k$, which means

$$mq_w = w^\alpha \Gamma(1 - \alpha) (1 + o(1)) = k, \tag{S17}$$

so that

$$w = k^{1/\alpha} \Gamma(1 - \alpha)^{-1/\alpha} (1 + o(1)). \tag{S18}$$

This implies that, with $m = n - 1$,

$$\begin{aligned}\mathbb{E}[N_k] &= n \mathbb{E} [\mathbb{P}(D_1 = k \mid W_1)] \\ &= (1 + o(1))n \int_1^\infty \frac{1}{\sqrt{2\pi m q_w(1 - q_w)}} e^{-(k - m q_w)^2 / [2m q_w(1 - q_w)]} \frac{\alpha}{w^{\alpha+1}} dw \\ &= (1 + o(1)) \int_1^\infty \frac{1}{\sqrt{2\pi n q_w}} e^{-(k - n q_w)^2 / [2n q_w]} \frac{\alpha}{w^{\alpha+1}} dw,\end{aligned}\tag{S19}$$

as long as $n q_w \gg 1$, and thus, since $k \approx n q_w$, also $k \gg 1$. Since the above integral is dominated by $n q_w$ that are close to k , we may replace $n q_w$ by k everywhere, except in the $(k - n q_w)^2$ term. This gives

$$\mathbb{E}[N_k] = (1 + o(1)) \frac{n}{\sqrt{2\pi k}} \int_1^\infty e^{-(k - n q_w)^2 / [2k]} \frac{\alpha}{w^{\alpha+1}} dw.\tag{S20}$$

We next substitute $n q_w \approx w^\alpha \Gamma(1 - \alpha)$ to arrive at

$$\begin{aligned}\mathbb{E}[N_k] &= (1 + o(1)) \frac{n}{\sqrt{2\pi k}} \int_1^\infty e^{-(k - w^\alpha \Gamma(1 - \alpha))^2 / [2k]} \frac{\alpha}{w^{\alpha+1}} dw \\ &= (1 + o(1)) \frac{n\alpha}{w_k^{\alpha+1} \sqrt{2\pi k}} \int_1^\infty e^{-(k - w^\alpha \Gamma(1 - \alpha))^2 / [2k]} dw,\end{aligned}\tag{S21}$$

where w_k solves $w^\alpha \Gamma(1 - \alpha) = k$, and thus

$$w_k = k^{1/\alpha} \Gamma(1 - \alpha)^{-1/\alpha}.\tag{S22}$$

We then let $z = w^\alpha \Gamma(1 - \alpha)$, so that $dz = \alpha w^{\alpha-1} \Gamma(1 - \alpha) dw$, so that

$$dw = \Gamma(1 - \alpha)^{-1} (z / \Gamma(1 - \alpha))^{(1-\alpha)/\alpha} dz = z^{(1-\alpha)/\alpha} \Gamma(1 - \alpha)^{-1/\alpha} dz,\tag{S23}$$

so that

$$\begin{aligned}\mathbb{E}[N_k] &= (1 + o(1)) \frac{n\alpha}{w_k^{\alpha+1} \sqrt{2\pi k}} \int_1^\infty e^{-(k-z)^2 / [2k]} z^{(1-\alpha)/\alpha} \Gamma(1 - \alpha)^{-1/\alpha} dz \\ &= (1 + o(1)) \frac{n\alpha}{w_k^{\alpha+1} \sqrt{2\pi k}} \Gamma(1 - \alpha)^{-1/\alpha} k^{(1-\alpha)/\alpha} \int_1^\infty e^{-(k-z)^2 / [2k]} dz \\ &= (1 + o(1)) \frac{n\alpha}{w_k^{\alpha+1} \sqrt{2\pi k}} k^{(1-\alpha)/\alpha} \Gamma(1 - \alpha)^{-1/\alpha} \sqrt{2\pi k} \\ &= n(1 + o(1)) \alpha k^{-(\alpha+1)/\alpha} \Gamma(1 - \alpha)^{(\alpha+1)/\alpha} k^{(1-\alpha)/\alpha} \Gamma(1 - \alpha)^{-1/\alpha} \\ &= n(1 + o(1)) \frac{\alpha \Gamma(1 - \alpha)}{k^2}.\end{aligned}\tag{S24}$$

This confirms that $\mathbb{E}[N_k] = \Theta(1)$ when $k = \Theta(\sqrt{n})$, so that one cannot expect that $N_k / \mathbb{E}[N_k] \xrightarrow{P} 1$ for such values of k .

Since (S13) depends on k , for k large, in a relatively weak way, this means that, for values of w close to w_k ,

$$\mathbb{P}(D'_1 = k - 2 \mid W_1 = w) \approx \mathbb{P}(D_1 = k \mid W_1 = w).\tag{S25}$$

Thus, since such factors appear both in $\mathbb{E}[N_k]$ and $\mathbb{E} \left[\sum_{v \in [n]} \Delta_v \mathbb{1}_{D_v = k} \right]$, they cancel out asymptotically, so that

$$\frac{\mathbb{E} \left[\sum_{v \in [n]} \Delta_v \mathbb{1}_{D_v = k} \right]}{\mathbb{E}[N_k]} \approx n \binom{n-1}{2} \mathbb{P}(I_{1,2} I_{1,3} I_{2,3} = 1 \mid W_1 = w_k).\tag{S26}$$

Recalling (S4), this then shows that

$$\bar{C}_n(k) = (1 + o(1)) \frac{\binom{n-1}{2}}{\binom{k}{2}} \mathbb{P}(I_{1,2} I_{1,3} I_{2,3} = 1 \mid W_1 = w_k).\tag{S27}$$

We now take $k = a\sqrt{n}$, and obtain

$$\bar{C}_n(a\sqrt{n}) = (1 + o(1)) \frac{n\alpha^2}{a^2} \int_1^\infty \int_1^\infty [1 - e^{-xw_k/n^{1/\alpha}}][1 - e^{-yw_k/n^{1/\alpha}}][1 - e^{-xy/n^{1/\alpha}}](xy)^{-(\alpha+1)} dx dy. \quad (\text{S28})$$

We first note that, for $k = a\sqrt{n}$,

$$w_{a\sqrt{n}} = n^{1/(2\alpha)} a^{1/\alpha} \Gamma(1 - \alpha)^{-1/\alpha} \equiv n^{1/(2\alpha)} a^{1/\alpha} \tau_\alpha. \quad (\text{S29})$$

We rescale x and y by $n^{-1/2\alpha}$ to obtain

$$\begin{aligned} \bar{C}_n(a\sqrt{n}) &= (1 + o(1)) \frac{\alpha^2}{a^2} \int_{n^{-1/2\alpha}}^\infty \int_{n^{-1/2\alpha}}^\infty [1 - e^{-xa^{1/\alpha}\tau_\alpha}][1 - e^{-ya^{1/\alpha}\tau_\alpha}][1 - e^{-xy}](xy)^{-(\alpha+1)} dx dy \\ &= (1 + o(1)) \frac{\alpha^2}{a^2} \int_0^\infty \int_0^\infty [1 - e^{-xa^{1/\alpha}\tau_\alpha}][1 - e^{-ya^{1/\alpha}\tau_\alpha}][1 - e^{-xy}](xy)^{-(\alpha+1)} dx dy, \end{aligned} \quad (\text{S30})$$

as predicted in (S5). \square

S.II. ASYMPTOTICS OF THE CLUSTERING FUNCTION

Lemma 1 ($\bar{C}(a)$ is bounded by 1). *For all $a > 0$, $\bar{C}(a) \leq 1$.*

Proof. Estimating $1 - e^{-xy} \leq 1$ bounds $\bar{C}(a)$ by

$$\bar{C}(a) \leq \frac{\alpha^2}{a^2} \left(\int_0^\infty [1 - e^{-xa^{1/\alpha}\tau_\alpha}] x^{-(\alpha+1)} dx \right)^2, \quad (\text{S31})$$

for which we note that

$$\begin{aligned} \int_0^\infty [1 - e^{-xa^{1/\alpha}\tau_\alpha}] x^{-(\alpha+1)} dx &= \int_0^\infty \int_0^{xa^{1/\alpha}\tau_\alpha} e^{-y} dy x^{-(\alpha+1)} dx \\ &= \int_0^\infty e^{-y} \int_{ya^{-1/\alpha}/\tau_\alpha}^\infty x^{-(\alpha+1)} dx dy = \frac{1}{\alpha} \int_0^\infty e^{-y} (ya^{-1/\alpha}/\tau_\alpha)^{-\alpha} dy \\ &= \frac{a\tau_\alpha^\alpha}{\alpha} \int_0^\infty e^{-y} y^{-\alpha} dy = \frac{a\tau_\alpha^\alpha}{\alpha} \Gamma(1 - \alpha) \\ &= \frac{a}{\alpha}, \end{aligned} \quad (\text{S32})$$

using that $\tau_\alpha = \Gamma(1 - \alpha)^{-1/\alpha}$. Thus, indeed, $\bar{C}(a) \leq 1$. \square

We next investigate $\bar{C}(a)$ for $a \ll 1$:

Lemma 2 ($\bar{C}(a)$ is close to 1 for a small). *As $a \searrow 0$,*

$$\bar{C}(a) = 1 + o(1). \quad (\text{S33})$$

Proof. For $a \ll 1$, we write

$$\begin{aligned} \bar{C}(a) &= \frac{\alpha^2}{a^2} \int_0^\infty \int_0^\infty [1 - e^{-xa^{1/\alpha}\tau_\alpha}][1 - e^{-ya^{1/\alpha}\tau_\alpha}](xy)^{-(\alpha+1)} dx dy \\ &\quad - \frac{\alpha^2}{a^2} \int_0^\infty \int_0^\infty [1 - e^{-xa^{1/\alpha}\tau_\alpha}][1 - e^{-ya^{1/\alpha}\tau_\alpha}] e^{-xy} (xy)^{-(\alpha+1)} dx dy. \end{aligned} \quad (\text{S34})$$

The first integral equals 1 by Lemma 1, so that

$$\bar{C}(a) = 1 - \bar{C}_1(a), \quad (\text{S35})$$

where

$$\bar{C}_1(a) = \frac{\alpha^2}{a^2} \int_0^\infty \int_0^\infty [1 - e^{-xa^{1/\alpha}\tau_\alpha}][1 - e^{-ya^{1/\alpha}\tau_\alpha}] e^{-xy} (xy)^{-(\alpha+1)} dx dy. \quad (\text{S36})$$

We first bound the integrals where either x or y is in $[0, a^{-\varepsilon}]$, for some $\varepsilon > 0$ sufficiently small, as

$$\begin{aligned} & \frac{2\alpha^2}{a^2} \int_0^\infty \int_0^{a^{-\varepsilon}} [1 - e^{-xa^{1/\alpha}\tau_\alpha}][1 - e^{-ya^{1/\alpha}\tau_\alpha}]e^{-xy}(xy)^{-(\alpha+1)} dx dy \\ & \leq \frac{2\alpha^2}{a^2} \int_0^\infty [1 - e^{-xa^{1/\alpha}\tau_\alpha}]x^{-(\alpha+1)} dx a^{1/\alpha} \int_0^{a^{-\varepsilon}} y^{-\alpha} dy \\ & \leq \frac{2\alpha}{a(\alpha-1)} a^{1/\alpha-\varepsilon(1-\alpha)} = o(1), \end{aligned} \quad (\text{S37})$$

using (S32) and the fact that $1/\alpha - \varepsilon(1-\alpha) > 1$ for $\varepsilon > 0$ sufficiently small since $\alpha \in (0, 1)$. Thus,

$$\bar{C}_1(a) = o(1) + \frac{\alpha^2}{a^2} \int_{a^{-\varepsilon}}^\infty \int_{a^{-\varepsilon}}^\infty [1 - e^{-xa^{1/\alpha}\tau_\alpha}][1 - e^{-ya^{1/\alpha}\tau_\alpha}]e^{-xy}(xy)^{-(\alpha+1)} dx dy, \quad (\text{S38})$$

which is bounded by $e^{-a^{-2\varepsilon}} = o(1)$. This shows that $\bar{C}_1(a) = o(1)$ for $a \searrow 0$, and thus proves that $\bar{C}(a) = 1 + o(1)$. \square

For $a \rightarrow \infty$, the integral should be dominated by small x, y , so that one might consider to expand $1 - e^{-xy} = xy$, to obtain

$$\begin{aligned} \bar{C}(a) &= (1 + o(1)) \frac{\alpha^2}{a^2} \int_0^\infty \int_0^\infty [1 - e^{-xa^{1/\alpha}\tau_\alpha}][1 - e^{-ya^{1/\alpha}\tau_\alpha}](xy)^{-\alpha} dx dy \\ &= (1 + o(1)) \frac{\alpha^2}{a^2} (a^{1/\alpha}\tau_\alpha)^{2\alpha-2} \left(\int_0^\infty [1 - e^{-x}]x^{-\alpha} dx \right)^2. \end{aligned} \quad (\text{S39})$$

However, the integral that is squared is infinite, so that we need to proceed alternatively. In fact, this analysis is quite intricate, and a careful split is necessary. The main result is as follows:

Lemma 3 (Large a asymptotics of $\bar{C}(a)$). *As $a \nearrow \infty$,*

$$\bar{C}(a) = 2\Gamma(1-\alpha) \frac{\log a}{a^2} + O(a^{-2}). \quad (\text{S40})$$

Proof. We again split the integral conveniently. We split the integral depending on whether x or y is in $[0, a^{-1/\alpha}/\tau_\alpha]$ or not. This gives

$$\bar{C}(a) = \bar{C}_1(a) + \bar{C}_2(a) + \bar{C}_3(a), \quad (\text{S41})$$

where

$$\bar{C}_1(a) = \frac{\alpha^2}{a^2} \int_{a^{-1/\alpha}/\tau_\alpha}^\infty \int_{a^{-1/\alpha}/\tau_\alpha}^\infty [1 - e^{-xa^{1/\alpha}\tau_\alpha}][1 - e^{-ya^{1/\alpha}\tau_\alpha}][1 - e^{-xy}](xy)^{-(\alpha+1)} dx dy, \quad (\text{S42})$$

$$\bar{C}_2(a) = \frac{\alpha^2}{a^2} \int_0^{a^{-1/\alpha}/\tau_\alpha} \int_0^{a^{-1/\alpha}/\tau_\alpha} [1 - e^{-xa^{1/\alpha}\tau_\alpha}][1 - e^{-ya^{1/\alpha}\tau_\alpha}][1 - e^{-xy}](xy)^{-(\alpha+1)} dx dy. \quad (\text{S43})$$

We bound, again using (S32) and $1 - e^{-xy} \leq xy$,

$$\begin{aligned} \bar{C}_2(a) &\leq \frac{\alpha^2}{a^2} \int_0^{a^{-1/\alpha}/\tau_\alpha} \int_0^{a^{-1/\alpha}/\tau_\alpha} [1 - e^{-xa^{1/\alpha}\tau_\alpha}][1 - e^{-ya^{1/\alpha}\tau_\alpha}](xy)^{-\alpha} dx dy \\ &= \frac{\alpha^2}{a^2} \left(\int_0^{a^{-1/\alpha}/\tau_\alpha} y^{-\alpha} dy \right)^2 \\ &= \Theta(1) a^{-2} (a^{-1/\alpha})^{2(1-\alpha)} = o(a^{-2}). \end{aligned} \quad (\text{S44})$$

We continue with $\bar{C}_3(a)$, which is the most involved. We bound $1 - e^{-ya^{1/\alpha}\tau_\alpha} \leq ya^{1/\alpha}$ to obtain

$$\bar{C}_3(a) \leq \frac{2\alpha^2 a^{1/\alpha}}{a^2} \int_0^{a^{-1/\alpha}/\tau_\alpha} \int_{a^{-1/\alpha}/\tau_\alpha}^\infty (xy)^{-(\alpha+1)} y [1 - e^{-xy}] dx dy. \quad (\text{S45})$$

We bound $1 - e^{-xy} \leq (xy) \wedge 1$. The integral where $x \leq 1/y$ is bounded by

$$\Theta(1)a^{-2+1/\alpha} \int_0^{a^{-1/\alpha}/\tau_\alpha} y^{-\alpha+1} \int_0^{1/y} x^{-\alpha} dx dy \leq \Theta(1)a^{-2+1/\alpha} \int_0^{a^{-1/\alpha}/\tau_\alpha} dy \leq \Theta(1)a^{-2}. \quad (\text{S46})$$

Similarly, the integral where $x > 1/y$ is bounded by

$$\Theta(1)a^{-2+1/\alpha} \int_0^{a^{-1/\alpha}/\tau_\alpha} y^{-\alpha} \int_{1/y}^\infty x^{-(\alpha+1)} dx dy \leq \Theta(1)a^{-2+1/\alpha} \int_0^{a^{-1/\alpha}/\tau_\alpha} dy \leq \Theta(1)a^{-2}. \quad (\text{S47})$$

This shows that $\bar{C}_3(a) = O(a^{-2})$.

We finally compute $\bar{C}_1(a)$, which we rewrite as

$$\begin{aligned} \bar{C}_1(a) &= \alpha^2 \tau_\alpha^{2\alpha} \int_1^\infty \int_1^\infty [1 - e^{-x}][1 - e^{-y}][1 - e^{-xya^{-2/\alpha}/\tau_\alpha^2}](xy)^{-(\alpha+1)} dx dy \\ &= \tau_\alpha^{2\alpha} \mathbb{E}[1 - e^{-W_1 W_2 a^{-2/\alpha}/\tau_\alpha^2}] + \bar{e}_1(a), \end{aligned} \quad (\text{S48})$$

where we let $\bar{e}_1(a)$ denote the contribution due to e^{-x} and e^{-y} . We use [30, (4.6)], which states that

$$\mathbb{E}[1 - e^{-\delta W_1 W_2}] = (1 + o(1))\alpha\Gamma(1 - \alpha)\delta^\alpha \log(1/\delta). \quad (\text{S49})$$

This gives

$$\bar{C}_1(a) = \tau_\alpha^{2\alpha} \alpha \tau_\alpha^{-2\alpha} \frac{2}{\alpha} \Gamma(1 - \alpha) \frac{\log a}{a^2} + \bar{e}_1(a) = 2\Gamma(1 - \alpha) \frac{\log a}{a^2} + \bar{e}_1(a). \quad (\text{S50})$$

Finally,

$$\begin{aligned} \bar{e}_1(a) &\leq 2\alpha^2 \tau_\alpha^{2\alpha} \int_1^\infty \int_1^\infty e^{-x} [1 - e^{-xya^{-2/\alpha}/\tau_\alpha^2}](xy)^{-(\alpha+1)} dx dy \\ &= 2\tau_\alpha^{2\alpha} \mathbb{E}[e^{-W_1}(1 - e^{-W_1 W_2 a^{-2/\alpha}/\tau_\alpha^2})] = O(a^{-2}). \end{aligned} \quad (\text{S51})$$

This can be seen by letting X be defined by

$$\mathbb{P}(X \in [a, b]) = \frac{1}{\mathbb{E}[e^{-W_1}]} \mathbb{E}[e^{-W_1} \mathbb{1}_{\{X \in [a, b]\}}], \quad (\text{S52})$$

so that

$$\bar{e}_1(a) = \Theta(1) \mathbb{E}[1 - e^{-XW a^{-2/\alpha}/\tau_\alpha^2}]. \quad (\text{S53})$$

Since X has thin tails (it has an exponential moment), the random variable XW is regularly varying with exponent α , so that

$$\mathbb{E}[1 - e^{-XW a^{-2/\alpha}/\tau_\alpha^2}] = \Theta(a^{-2}), \quad (\text{S54})$$

as claimed. The above follows from the fact that XW is again heavy-tailed with tail exponent α , as proved in [39, Proposition 5.2]. \square

S.III. COMPUTATION OF AVERAGE CLUSTERING COEFFICIENT

The limiting asymptotics for hubs and leaves allows us to derive an estimate of the average clustering coefficient of the network \bar{C} . Indeed, one needs to integrate the annealed clustering function $\bar{C}(a)$ over the distribution $P(a)$ of the reduced degree a , and from Figure 1 it is clear that one can split the integral into the two leaf (L) and hub (H) regimes as

$$\bar{C} = \int_{a_{\min}}^\infty da \bar{C}(a) P(a) = \int_{a_{\min}}^{a^*} da \bar{C}_L(a) P(a) + \int_{a^*}^\infty da \bar{C}_H(a) P(a), \quad (\text{S55})$$

where $C_H(a) \sim 2\Gamma(1-\alpha)\frac{\log a}{a^2}$ (for $a > a^*$) is the asymptotic clustering function of hubs, while $C_L(a) \sim 1$ (for $a_{min} < a < a^*$) is the asymptotic plateau for leaves, a_{min} is the minimal reduced degree above which the clustering function starts to have meaning, and a^* is an appropriate crossover value between the two regimes. This crossover is visible in Figure 1, although its value is not easily identified. Luckily, as we will show in the following computations, the actual value of a^* is not necessary for the computation of the clustering to go through, and we can proceed without specifying it.

The main issue in the evaluation of the integral in (S55) is that the degree distribution is not known everywhere but only in the tail [30], where it has the asymptotic behaviour $\Gamma(1-\alpha)k^{-2}$. Transforming to the distribution $P(a)$ of the reduced degree $a = \frac{k}{\sqrt{n}}$,

$$P(a) \sim \frac{\Gamma(1-\alpha)}{\sqrt{n}} a^{-2}. \quad (\text{S56})$$

Nonetheless, the first integral can be evaluated by realizing that by definition it evaluates to the fraction of leaves nodes or, equivalently

$$\int_{a_{min}}^{a^*} da \bar{C}_L(a) P(a) = \int_{a_{min}}^{a^*} da P(a) = \begin{cases} 1 - \int_{a^*}^{\infty} da P(a) & \text{if } C_{k<2} \text{ undefined,} \\ 1 - r_{0/1} - \int_{a^*}^{\infty} da P(a) & \text{if } C_{k<2} = 0, \end{cases} \quad (\text{S57})$$

and the last term can be recomprised in the second integral as it is evaluated on the same interval, so that the average clustering coefficient has the expression

$$\bar{C} = \begin{cases} 1 + \int_{a^*}^{\infty} P(a)(\bar{C}_H(a) - 1) & \text{if } C_{k<2} \text{ undefined,} \\ 1 - r_{0/1} + \int_{a^*}^{\infty} da P(a)(\bar{C}_H(a) - 1) & \text{if } C_{k<2} = 0, \end{cases} \quad (\text{S58})$$

We can evaluate this last integral as

$$\begin{aligned} \int_{a^*}^{\infty} da P(a)(\bar{C}_H(a) - 1) &= \int_{a^*}^{\infty} da \left[2\Gamma(1-\alpha)\frac{\log a}{a^2} - 1 \right] \frac{\Gamma(1-\alpha)}{a^2\sqrt{n}} \\ &= \frac{\Gamma(1-\alpha)}{\sqrt{n}} \frac{6\Gamma(1-\alpha)\log a^* + 2\Gamma(1-\alpha) - 9(a^*)^2}{9(a^*)^3} \\ &= o(1), \end{aligned} \quad (\text{S59})$$

and see that it is suppressed by a square root of n term, whatever the value of a^* .

S.IV. COMPUTATION OF $r_{0/1}$

We start by computing the fraction of nodes that are disconnected from the graph as

$$r_0 \equiv \frac{1}{n} \sum_{i=1}^n \prod_{j: j \neq i} (1 - p_{ij}) = \frac{1}{n} \sum_{i=1}^n e^{-\delta_n w_i \sum_{j \neq i} w_j}, \quad (\text{S60})$$

where we recall that $\delta_n = n^{-1/\alpha}$. Since the $j = i$ term in the sum in the exponential makes little difference, we can approximate

$$r_0 \approx \frac{1}{n} \sum_{i=1}^n e^{-\delta_n w_i \sum_j w_j}. \quad (\text{S61})$$

We next use that most of the weights have normal size, and they contribute most to the sum over $i \in \{1, \dots, n\}$. Thus,

$$r_0 \approx \mathbb{E} \left[e^{-W S_n} \mid S_n \right], \quad (\text{S62})$$

where we take the expectation over the Pareto variable W in the above, we abbreviate

$$S_n = \delta_n \sum_{j=1}^n w_j, \quad (\text{S63})$$

and condition on this total rescaled weight. We note that the random variable S_n converges in distribution to an α -stable distribution, since the random variables $(w_i)_{i=1}^n$ are Pareto variables with infinite mean. Thus,

$$r_0 \approx \mathbb{E} \left[e^{-WS} \mid \mathcal{S} \right], \quad (\text{S64})$$

where \mathcal{S} is an α -stable random variable. Equation (S64) requires some interpretation. What it means is that the proportion of vertices with r_0 degree 0, given the vertex weights $(w_i)_{i=1}^n$, is close to the rhs of (S62), i.e., it holds that $r_0 \approx \mathbb{E} \left[e^{-WS_n} \mid S_n \right]$, where the rescaled total weight S_n is defined in (S63). In particular, this means that, when simulating the network several times (and thus redrawing the vertex weights), the proportion of vertices with degree 0 *fluctuates macroscopically*, even in the large graph limit. This is a type of *non-self-averaging* phenomenon that is rather unusual in network science. The simulations shown in Figures S1 S2 S3 confirm that (S64) is an excellent approximation of r_0 , and that it remains truly random in the large-graph limit. We can also use (S64) us to relate our approximation to [30, Proposition 4], in which $\mathbb{E}[r_0]$ is shown to be approximated by

$$\mathbb{E}[r_0] \approx \mathbb{E} \left[e^{-\Gamma(1-\alpha)W^\alpha} \right], \quad (\text{S65})$$

which indeed equals $\mathbb{E} \left[e^{-WS} \right]$, since, for every $a \geq 0$,

$$\mathbb{E} \left[e^{-aS} \right] = e^{-\Gamma(1-\alpha)a^\alpha}. \quad (\text{S66})$$

This follows from [30, Theorem 5]. For a practical computation of the approximation of r_0 , we use the fact, again for $a \geq 0$,

$$\mathbb{E} \left[e^{-aW} \right] = \alpha a^\alpha \Gamma(-\alpha, a), \quad (\text{S67})$$

where we recall that $\Gamma(r, a)$ is the incomplete gamma function. Applying this to (S62), we are led to

$$r_0 \approx \alpha S_n^\alpha \Gamma(-\alpha, S_n). \quad (\text{S68})$$

We show in Figures S1 S2 S3 that (S68) is in very good accordance with the actual fraction of disconnected nodes (central panels).

We extend the above analysis to the proportion r_1 of vertices of degree 1. We start from

$$\begin{aligned} r_1 &\equiv \frac{1}{n} \sum_{i,k: i \neq k} p_{ik} \prod_{j: j \neq i,k} (1 - p_{ij}) \\ &= \frac{1}{n} \sum_{i,k: i \neq k} (1 - e^{-\delta_n w_i w_k}) e^{-\delta_n w_i \sum_{j: j \neq i,k} w_j} \\ &\approx \sum_k \mathbb{E} \left[(1 - e^{-W \delta_n w_k}) e^{-W \delta_n \sum_{j: j \neq k} w_j} \right], \end{aligned} \quad (\text{S69})$$

where the asymptotics follows from the fact that the main contribution in the sum over i arises from normal weight vertices, so that the average over i can be replaced by an expectation with respect to W .

Note that the dominant contributions to the sum over k in (S69) correspond to those k for which w_k is of the order $1/\delta_n = n^{1/\alpha}$, which means that these are the maximal-weight vertices. This will be the guiding principle to derive the asymptotics of the above formula.

For simplicity, and without loss of generality, we will assume that the weights are *ordered* from large to small, so that $w_1 \geq w_2 \cdots \geq w_n$. We can rewrite

$$\delta_n \sum_{j: j \neq k} w_j = S_n - \delta_n w_k = S_n - y_k^{(n)}, \quad (\text{S70})$$

where we recall S_n from (S63), and we define the rescaled vertex weights $(y_k^{(n)})_{k \geq 1}$ as

$$y_k^{(n)} = \delta_n w_k. \quad (\text{S71})$$

In terms of these definitions, we obtain the finite-size approximation

$$r_1 \approx \sum_k \mathbb{E} \left[(1 - e^{-W y_k^{(n)}}) e^{-W(S_n - y_k^{(n)})} \mid (y_k^{(n)})_{k \geq 1} \right]. \quad (\text{S72})$$

This approximation is inspired by the asymptotics properties of r_1 . Indeed, as $n \rightarrow \infty$, we have the convergence in distribution

$$\left(S_n, (y_k^{(n)})_{k \geq 1} \right) \xrightarrow{d} \left(\sum_{j \geq 1} \Gamma_j^{-1/\alpha}, (\Gamma_k^{-1/\alpha})_{k \geq 1} \right), \quad (\text{S73})$$

where \xrightarrow{d} denotes convergence in distribution in the product topology, $(\Gamma_k)_{k \geq 1}$ are gamma random variables, i.e.,

$$\Gamma_k = \sum_{i=1}^k E_i, \quad (\text{S74})$$

where $(E_i)_{i \geq 1}$ are independent and identically distributed exponential random variables with mean 1. Because of this, we see that the random variables in (S72) converge in distribution in the large graph limit, so that

$$r_1 \xrightarrow{d} \sum_k \mathbb{E} \left[(1 - e^{-W y_k}) e^{-W(S - y_k)} \mid (y_k)_{k \geq 1} \right], \quad (\text{S75})$$

where

$$\left(\mathcal{S}, (y_k)_{k \geq 1} \right) \equiv \left(\sum_{j \geq 1} \Gamma_j^{-1/\alpha}, (\Gamma_k^{-1/\alpha})_{k \geq 1} \right). \quad (\text{S76})$$

Thus, as for r_0 , also r_1 converges in *distribution*, but it remains to fluctuate even in the large graph limit.

For a practical computation of the approximation of r_0 , we again use (S67) on the representation

$$r_1 \approx \sum_{k=1}^n \mathbb{E} \left[e^{-W(S_n - y_k^{(n)})} - e^{-W S_n} \mid (y_k^{(n)})_{k \geq 1} \right], \quad (\text{S77})$$

to arrive at

$$r_1 \approx \alpha \sum_{k=1}^n \left[(S_n - y_k^{(n)})^\alpha \Gamma(-\alpha, S_n - y_k^{(n)}) - S_n^\alpha \Gamma(-\alpha, S_n) \right], \quad (\text{S78})$$

which has the advantage that it no longer contains the expectation with respect to W . We show in Figures S1 S2 S3 that (S78) is in very good accordance with the actual fraction of disconnected nodes (bottom panels).

S.V. EXTENSION TO STABLE WEIGHTS

In this section we briefly discuss how our results can be extended to the case in which the weights are sampled from a genuine α -stable distribution $\tilde{\rho}_\alpha(w)$ with positive support and diverging mean. Throughout, we follow the formalism introduced in [37], and in particular we adopt the first parametrization defined there, corresponding to $k = 0$.

For stable laws, our arguments can be adapted by replacing the exact expression for the Pareto weight density, $\rho_\alpha(w) = \alpha w^{-(\alpha+1)}$ for $w \geq 1$ in (S1), with an asymptotic relation. Specifically, Theorem 1.2 of [37] shows that the density of an α -stable law satisfies

$$\tilde{\rho}_\alpha(w) = (1 + o(1)) \frac{\alpha \gamma^\alpha (1 + \beta) c_\alpha}{w^{\alpha+1}}, \quad w \geq 1, \quad (\text{S79})$$

where the tail parameter satisfies $\alpha \in (0, 1)$, $c_\alpha = \frac{\Gamma(\alpha)}{\pi} \sin(\frac{\pi\alpha}{2})$, γ denotes the scale parameter, and β is the skewness parameter of the stable distribution.

In order to work with a distribution supported on the positive real axis, we choose $\beta = 1$ and set the infimum of the support to zero. This choice fixes the location parameter to be $\delta = \gamma \tan(\frac{\pi\alpha}{2})$. The only remaining free parameter is therefore the scale γ , which we determine by requiring that the tails of the stable and Pareto distributions coincide asymptotically. Imposing this matching condition yields

$$\gamma = \left[\frac{\pi}{2 \Gamma(\alpha) \sin(\frac{\pi\alpha}{2})} \right]^{1/\alpha}. \quad (\text{S80})$$

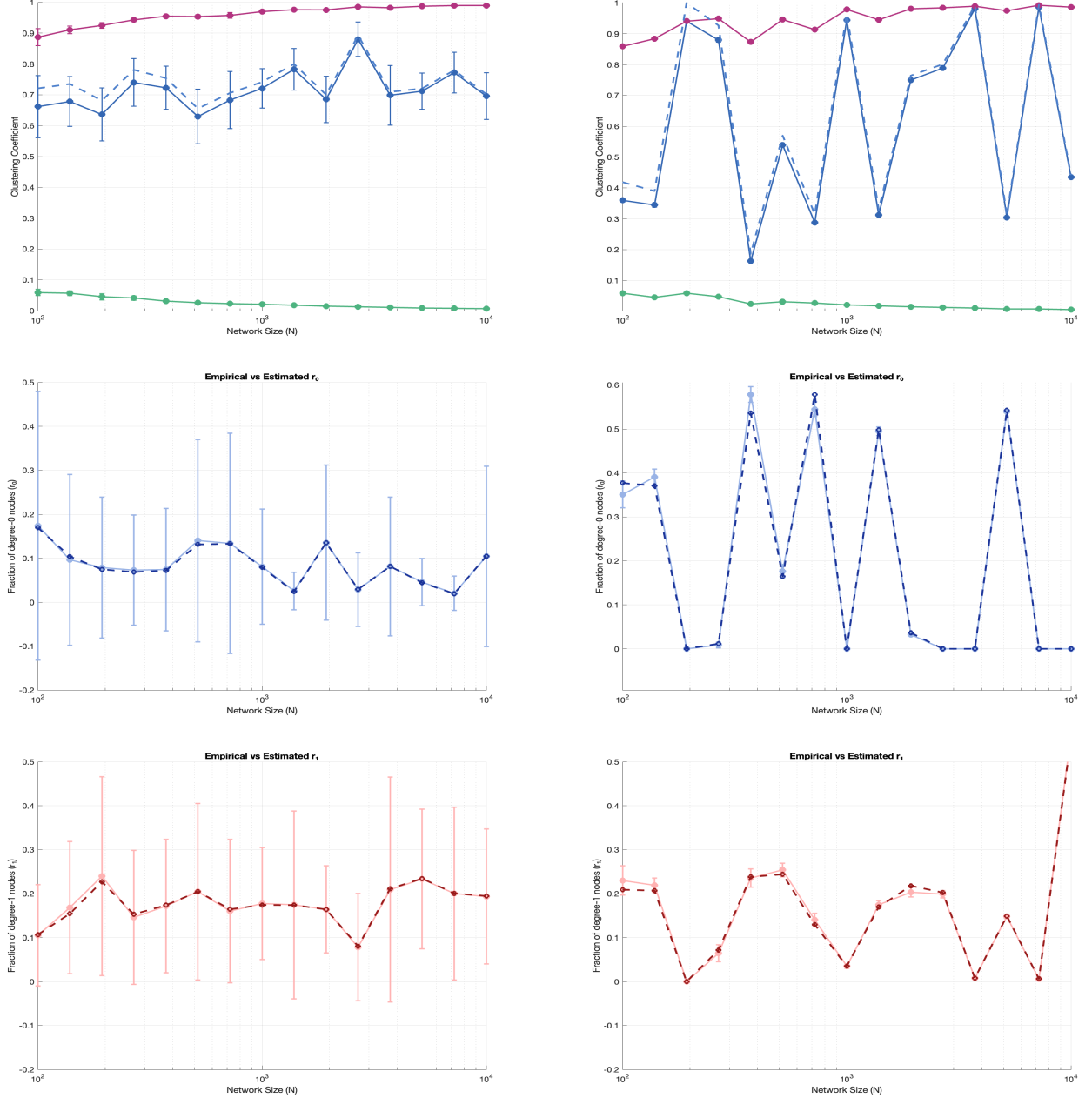


FIG. S1: Average local clustering coefficient C and distance to $r_{0/1}$ versus network size n (for $\alpha = 0.3$).

On the left, simulations are done by resampling weights every time an actual network is realized (sample of 10), while on the right for each n weights are extracted only once, and 10 different adjacency matrices are realized from the same weights. On top we show the node-averaged local clustering coefficient C , both including (blue symbols) and excluding (purple symbols) nodes with degree $k = 0, 1$ (note that the latter evolves smoothly towards 1 with shrinking error bars as n increases, while the former fluctuates with non-vanishing error bars, as a result of non-self-averaging). The dashed blue line is 1 minus the average of $r_{0/1}$ over realizations. Finally, in green the difference between $1 - r_{0/1}$ and C computed including nodes with $k < 2$ (notice the shrinking error bars). In the middle, the light blue line with error bars is the actual value of r_0 , while the dashed darker one is the approximation we derive in (S68). At the bottom, the light red line with error bars is the actual value of r_1 , while the dashed darker one is the approximation we derive in (S72).

With this choice of parameters, all the results we derived for Pareto-distributed weights extend directly to the case of stable sampling. In particular, since the integrals appearing in Section S.I are dominated by contributions from

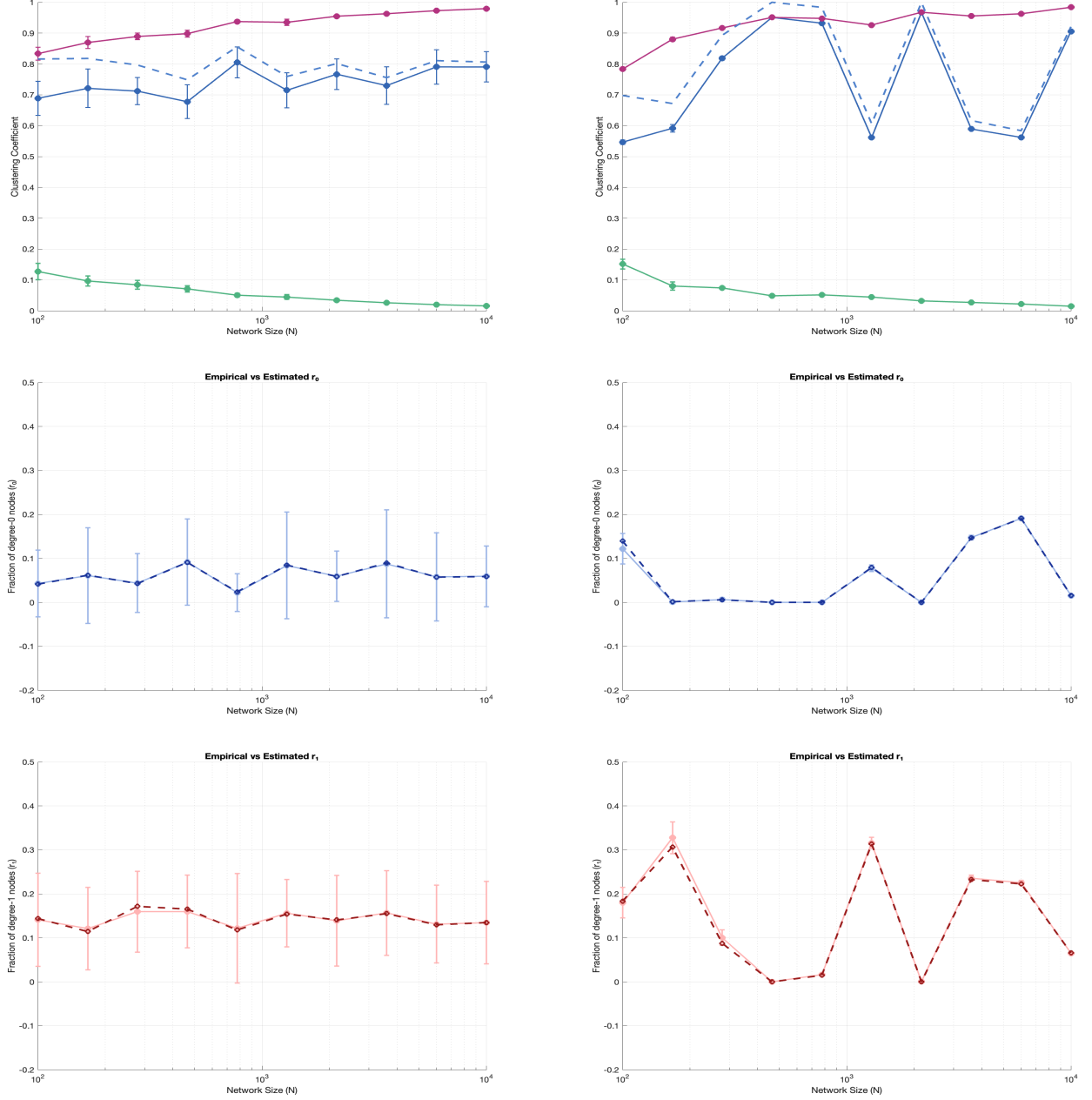


FIG. S2: **Average local clustering coefficient C and distance to $r_{0/1}$ versus network size n (for $\alpha = 0.5$).**

On the left, simulations are done by resampling weights every time an actual network is realized (sample of 10), while on the right for each n weights are extracted only once, and 10 different adjacency matrices are realized from the same weights. On top we show the node-averaged local clustering coefficient C , both including (blue symbols) and excluding (purple symbols) nodes with degree $k = 0, 1$ (note that the latter evolves smoothly towards 1 with shrinking error bars as n increases, while the former fluctuates with non-vanishing error bars, as a result of non-self-averaging). The dashed blue line is 1 minus the average of $r_{0/1}$ over realizations. Finally, in green the difference between $1 - r_{0/1}$ and C computed including nodes with $k < 2$ (notice the shrinking error bars). In the middle, the light blue line with error bars is the actual value of r_0 , while the dashed darker one is the approximation we derive in (S68). At the bottom, the light red line with error bars is the actual value of r_1 , while the dashed darker one is the approximation we derive in (S72).

large values of w , the asymptotic estimates derived in Section S.II remain valid. Similarly, the arguments used in Section S.IV to compute the fraction of disconnected nodes and nodes of degree one carry over almost verbatim to

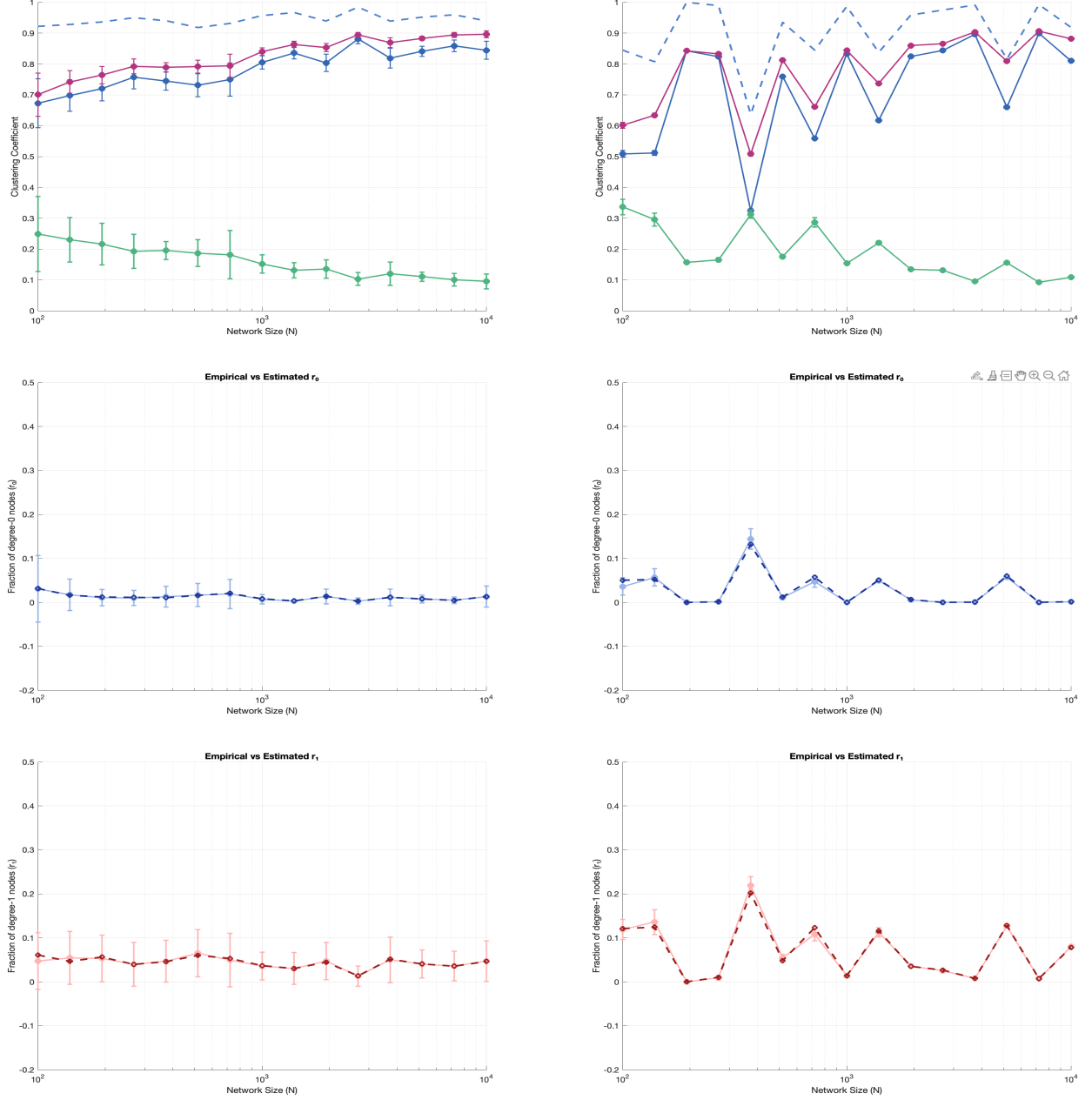


FIG. S3: **Average local clustering coefficient C and distance to $r_{0/1}$ versus network size n (for $\alpha = 0.7$).**

On the left, simulations are done by resampling weights every time an actual network is realized (sample of 10), while on the right for each n weights are extracted only once, and 10 different adjacency matrices are realized from the same weights. On top we show the node-averaged local clustering coefficient C , both including (blue symbols) and excluding (purple symbols) nodes with degree $k = 0, 1$ (note that the latter evolves smoothly towards 1 with shrinking error bars as n increases, while the former fluctuates with non-vanishing error bars, as a result of non-self-averaging). The dashed blue line is 1 minus the average of $r_{0/1}$ over realizations. Finally, in green the difference between $1 - r_{0/1}$ and C computed including nodes with $k < 2$ (notice the shrinking error bars). In the middle, the light blue line with error bars is the actual value of r_0 , while the dashed darker one is the approximation we derive in (S68). At the bottom, the light red line with error bars is the actual value of r_1 , while the dashed darker one is the approximation we derive in (S72).

the stable case. The only modification is the appearance of a constant c in (S73), which is now directly related to the scale parameter of the underlying stable law.

Indeed, in the convergence statement (S73), the partial sum S_n has a strictly α -stable distribution for every n . Interpreting S_n as the value at time 1 of a stable Lévy process, the sum $c \sum_{j \geq 1} \Gamma_j^{-1/\alpha}$ can be viewed as the collection of jump sizes of the process, ordered by decreasing magnitude. Correspondingly, the rescaled weights $n^{-1/\alpha} W_i$ represent the increments of the process over the time intervals $[(i-1)/n, i/n]$, and the variables $(y_k^{(n)})_{k=1}^n$ in (S71) can be interpreted as the ordered increments over these intervals. Since, with high probability and for large n , each interval contains at most one large jump, it follows that (S73) continues to hold in this setting, with the first coordinate (corresponding to the sum) having exactly the same distribution as in the Pareto case.

Finally, in Figures S5, S6, S7, and S8, we provide numerical evidence confirming that the results presented in the main text remain valid when the weights are drawn from an α -stable distribution, in agreement with the arguments given above.

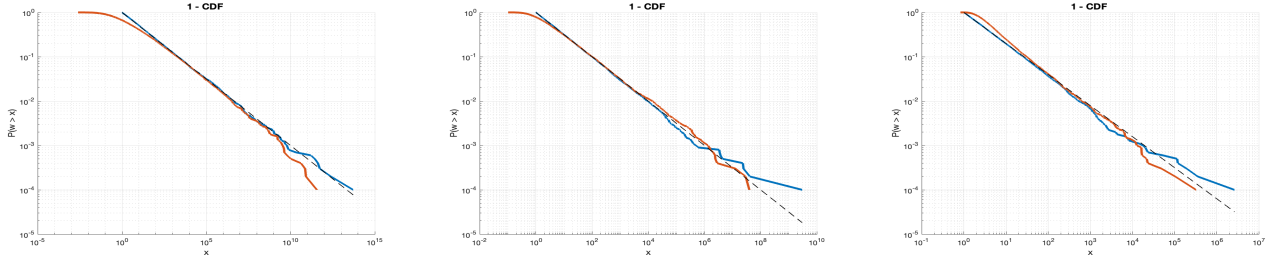


FIG. S4: **Comparison between pure Pareto and Stable distributions in the tail behaviour.** Using the parameter of (S80), we can match the tails of the two distributions. From left to right $\alpha = 0.3, 0.5, 0.7$, sample of 10^4 .

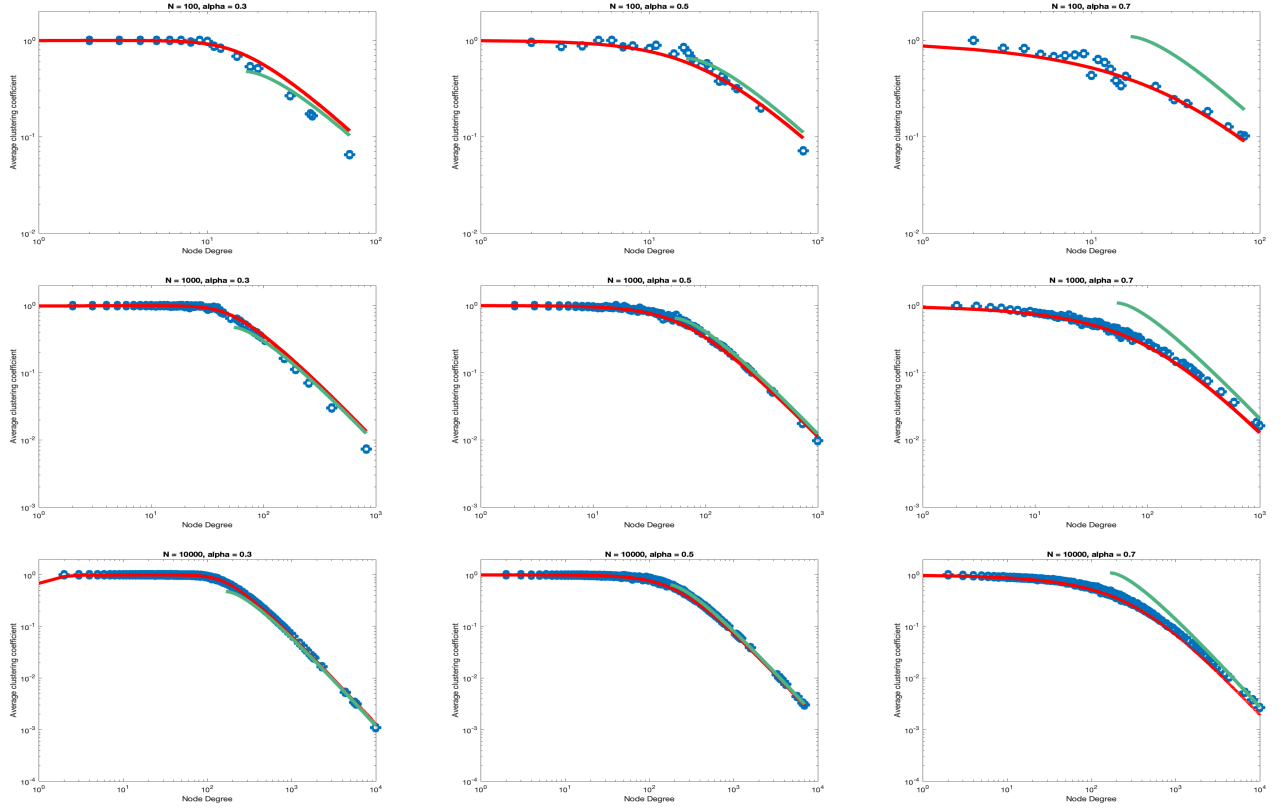


FIG. S5: Clustering functions for different values of n and α for the MSM model (1) with Stable weights (S79). Blue circles: empirical clustering function (4) (versus the reduced degree $a = k/\sqrt{n}$) computed on actual realized graphs sampled from the model (obtained by sampling the weights once, and sampling the graph once conditionally on the realized weights). Red curves: our analytical expression (6) for the annealed clustering function. Green curves: our asymptotic calculation (8) valid for diverging reduced degrees. We evaluate and plot all functions only for degrees larger than 1, to avoid ambiguities in the definition of the clustering coefficient for $k < 2$. From top to bottom: $n = 10^2, 10^3, 10^4$. From left to right: $\alpha = 0.3, 0.5, 0.7$.

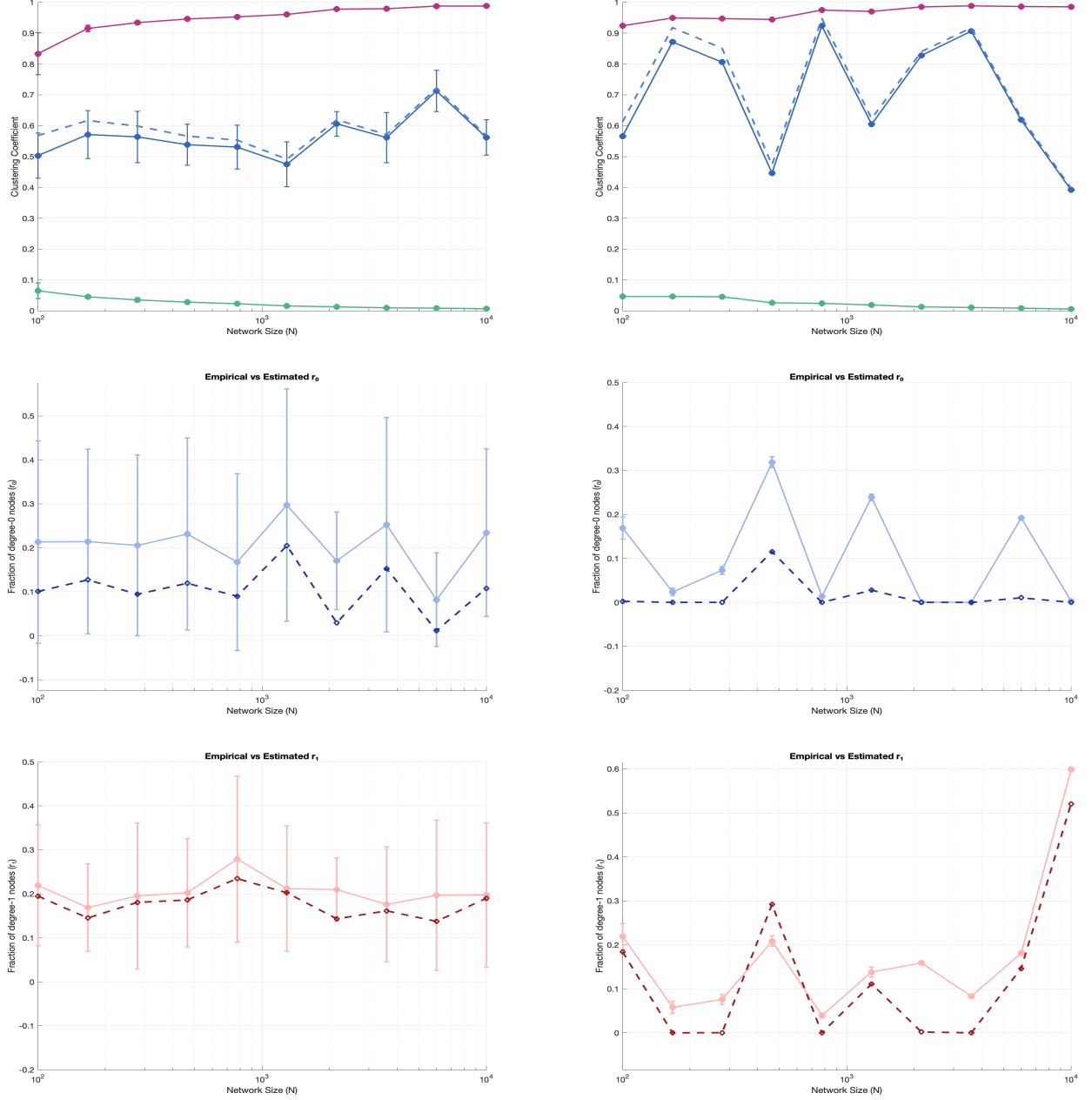


FIG. S6: Average local clustering coefficient C and distance to $r_{0/1}$ versus network size n , with weights drawn from a Stable distribution (for $\alpha = 0.3$). On the left, simulations are done by resampling weights every time an actual network is realized (sample of 10), while on the right for each n weights are extracted only once, and 10 different adjacency matrices are realized from the same weights. On top we show the node-averaged local clustering coefficient C , both including (blue symbols) and excluding (purple symbols) nodes with degree $k = 0, 1$ (note that the latter evolves smoothly towards 1 with shrinking error bars as n increases, while the former fluctuates with non-vanishing error bars, as a result of non-self-averaging). The dashed blue line is 1 minus the average of $r_{0/1}$ over realizations. Finally, in green the difference between $1 - r_{0/1}$ and C computed including nodes with $k < 2$ (notice the shrinking error bars). In the middle, the light blue line with error bars is the actual value of r_0 , while the dashed darker one is the approximation we derive in (S68). At the bottom, the light red line with error bars is the actual value of r_1 , while the dashed darker one is the approximation we derive in (S72).

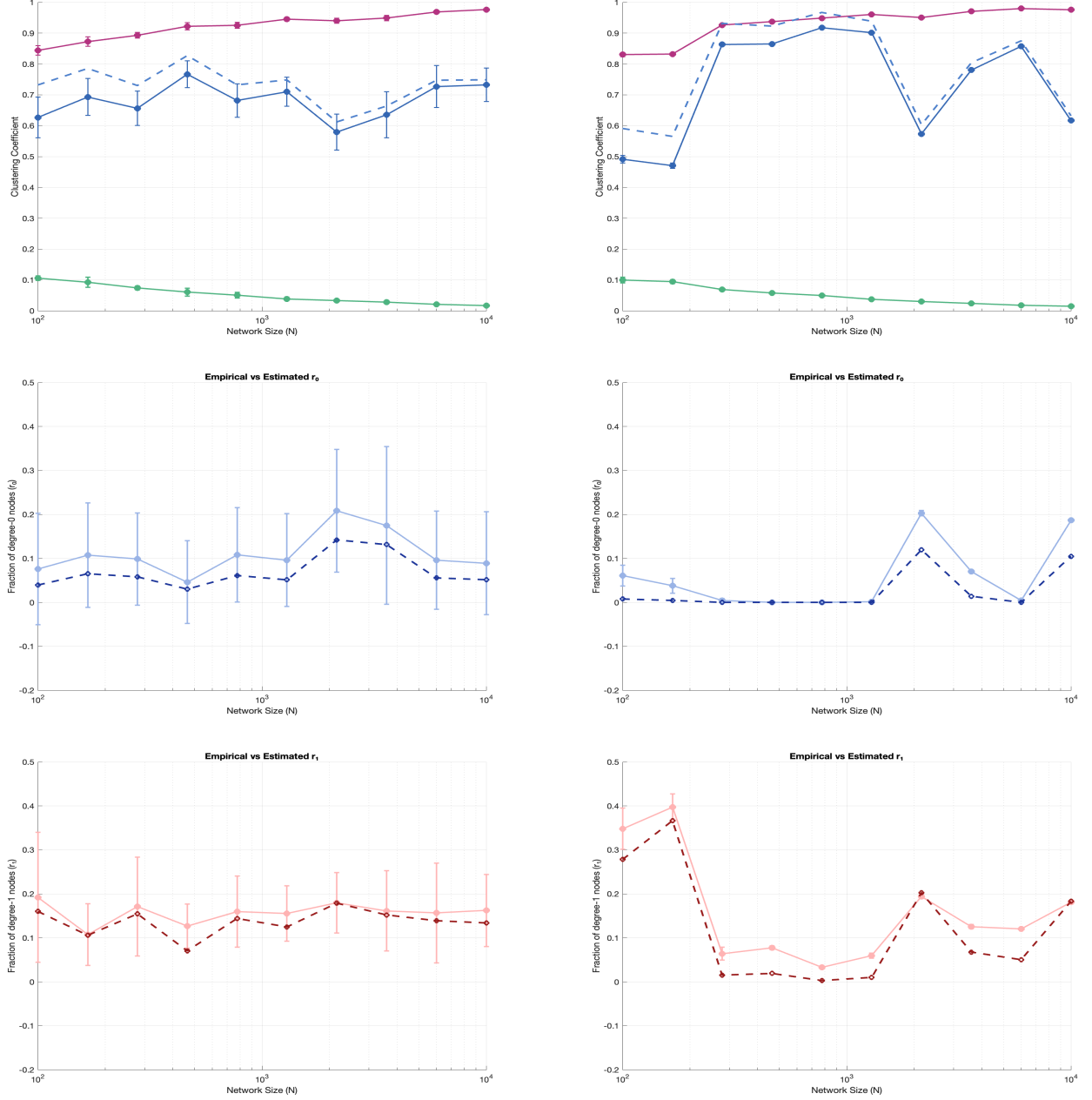


FIG. S7: Average local clustering coefficient C and distance to $r_{0/1}$ versus network size n , with weights drawn from a Stable distribution (for $\alpha = 0.5$). On the left, simulations are done by resampling weights every time an actual network is realized (sample of 10), while on the right for each n weights are extracted only once, and 10 different adjacency matrices are realized from the same weights. On top we show the node-averaged local clustering coefficient C , both including (blue symbols) and excluding (purple symbols) nodes with degree $k = 0, 1$ (note that the latter evolves smoothly towards 1 with shrinking error bars as n increases, while the former fluctuates with non-vanishing error bars, as a result of non-self-averaging). The dashed blue line is 1 minus the average of $r_{0/1}$ over realizations. Finally, in green the difference between $1 - r_{0/1}$ and C computed including nodes with $k < 2$ (notice the shrinking error bars). In the middle, the light blue line with error bars is the actual value of r_0 , while the dashed darker one is the approximation we derive in (S68). At the bottom, the light red line with error bars is the actual value of r_1 , while the dashed darker one is the approximation we derive in (S72).

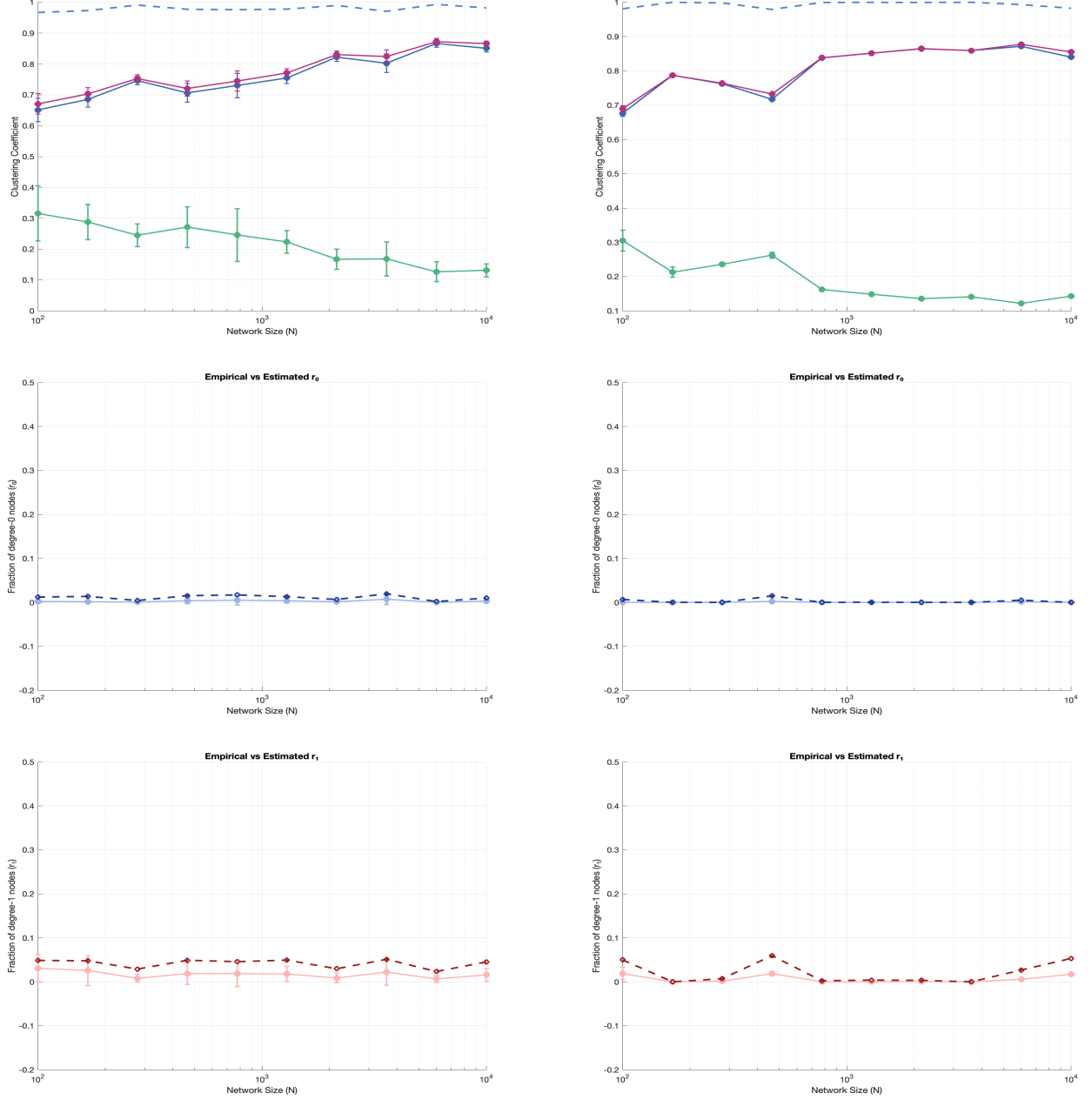


FIG. S8: Average local clustering coefficient C and distance to $r_{0/1}$ versus network size n , with weights drawn from a Stable distribution (for $\alpha = 0.7$). On the left, simulations are done by resampling weights every time an actual network is realized (sample of 10), while on the right for each n weights are extracted only once, and 10 different adjacency matrices are realized from the same weights. On top we show the node-averaged local clustering coefficient C , both including (blue symbols) and excluding (purple symbols) nodes with degree $k = 0, 1$ (note that the latter evolves smoothly towards 1 with shrinking error bars as n increases, while the former fluctuates with non-vanishing error bars, as a result of non-self-averaging). The dashed blue line is 1 minus the average of $r_{0/1}$ over realizations. Finally, in green the difference between $1 - r_{0/1}$ and C computed including nodes with $k < 2$ (notice the shrinking error bars). In the middle, the light blue line with error bars is the actual value of r_0 , while the dashed darker one is the approximation we derive in (S68). At the bottom, the light red line with error bars is the actual value of r_1 , while the dashed darker one is the approximation we derive in (S72).